Am J Cancer Res 2023;13(10):4579-4596
www.ajcr.us /ISSN:2156-6976/ajcr0151725

Original Article

GALNT5 functions as a suppressor of ferroptosis and a predictor of poor prognosis in pancreatic adenocarcinoma

Jiayi Yan[1*], Haiyi Gong[2*], Shuai Han[3*], Jialiang Liu[2], Zhipeng Wu[2], Zhenhua Wang[4], Ting Wang[2]

[1]International Peace Maternity and Child Health Hospital, School of Medicine, Shanghai Jiao Tong University, Shanghai, China; [2]Department of Orthopedic Oncology, Shanghai Changzheng Hospital, Naval Medical University, Shanghai, China; [3]Department of Orthopedics, Shanghai Pudong New Area People's Hospital, Shanghai, China; [4]Department of Laboratory Medicine, Shanghai Changzheng Hospital, Naval Medical University, Shanghai, China. [*]Equal contributors and co-senior authors.

Received June 12, 2023; Accepted August 22, 2023; Epub October 15, 2023; Published October 30, 2023

Abstract: Mucin-type O-glycosylation, a posttranslational modification of membrane and secretory proteins, facilitates metastasis and immune escape in tumor cells. N-acetylgalactosaminyl-transferase 5 (GALNT5), the enzyme initiating mucin-type O-glycosylation, is known to advance the progression of various tumors. Yet, the comprehensive role of GALNT5 in pan-cancer scenarios remains to be elucidated. In this research, we conducted a database-centric pan-cancer expression analysis of GALNT5. We examined its aberrant expression, assessed its prognostic implications, and explored the correlations between GALNT5 expression and factors such as ferroptosis, immune cell infiltration levels, and immune checkpoint gene expression across multiple tumor types. To substantiate GALNT5's role, we analyzed cell proliferation, migration, invasion, and ferroptosis in PAAD cells after GALNT5 knockdown. Additionally, RNA-seq was employed to discern potential downstream pathways influenced by GALNT5. Our findings indicate that GALNT5 expression is heightened in the majority of tumors, correlating with the prognosis of multiple cancers. There's a notable association between GALNT5 levels and ferroptosis-related genes, immune cell infiltration, and immune checkpoint genes. In PAAD specifically, the role of GALNT5 was further probed. Knockdown of GALNT5 curtailed the proliferation, migration, and invasion capacities of PAAD cells, concurrently promoting ferroptosis. Moreover, in vivo studies demonstrated that GALNT5 inhibition stunted PAAD tumor growth. The RNA-seq analysis unveiled inflammation and immune-centric pathways, such as the TNF signaling pathway, as potential downstream conduits of GALNT5. In conclusion, our pan-cancer study underscores GALNT5 as a potential therapeutic target for enhancing PAAD prognosis, given its strong ties with ferroptosis and immune cell infiltration. Our experiments further define GALNT5 as a novel suppressor of ferroptosis.

Keywords: GALNT5, pan-cancer, pancreatic adenocarcinoma, ferroptosis, immune microenvironment

Introduction

Cancer represents a substantial threat to human health globally, with its incidence steadily rising [1]. Despite significant advancements in treatments such as surgical resection, combined postoperative neoadjuvant chemoradiotherapy, molecular-targeted therapy, and immunotherapy, the intricate nature of tumor progression and resistance to therapies mean that only a few malignancies are fully curable [2]. PAAD, for instance, constitutes approximately 3% of all new cancer diagnoses and has a bleak 5-year survival rate of only 11% [3]. Leveraging big data can offer insights into the molecular underpinnings of tumorigenesis and progression. Specifically, pan-cancer analysis aids in discerning the interplay between genes and tumor-associated factors across different cancer types, providing the corresponding biological targets for tumor diagnosis and treatment.

Mucin-type O-glycosylation, a prevalent post-translational protein modification, has been associated with malignancy, especially with increased levels of truncated O-glycans like the Tn antigen [4, 5]. Tn antigen emerges from aber-

rant initiation of N-acetylgalactosamine (GalNAc)-type O-glycosylation [6, 7], and its elevated presence in human cancers promotes both metastasis and immune evasion [8, 9]. This modification is orchestrated by the 20 isoenzymes of polypeptide GalNAc transferases (GALNTs). Deviations in GALNT expression patterns have been linked to cancer stemness and metastasis in numerous malignancies [5, 10]. Notably, GALNT5, a GALNT member, has surfaced as a marker of poor prognosis in diverse tumors, such as hepatocellular carcinoma and cholangiocarcinoma [11-13]. Moreover, GALNT5 is one of the prominently downregulated genes in ferroptosis [14]. However, its exact role and mechanism remain elusive.

Introduced in 2012, ferroptosis, characterized by ferrous ion accumulation and lipid peroxidation, has emerged as a promising antitumor strategy [15]. Recent studies highlight its pivotal role in antitumor immunity and modulating the immune response to immune checkpoint (ICP) inhibition [16]. Furthermore, it is noteworthy that immunotherapy has been observed to enhance ferroptosis by augmenting lipid peroxide and iron within tumor cells, consequently influencing therapeutic efficacy [17]. This prompts speculation about GALNT5's potential involvement in ferroptosis and the immune microenvironment (IME).

Our study aims to examine GALNT5 expression across various tumors and discern its association with prognosis, ferroptosis, and IME using RNA-seq data from The Cancer Genome Atlas (TCGA). Considering the significant correlation between GALNT5 expression and PAAD patient prognosis, we also aim to understand GALNT5's influence on PAAD cell behaviors such as proliferation, migration, invasion, apoptosis, and ferroptosis. Subsequently, our objective is to elucidate GALNT5-associated mechanisms in PAAD cells via RNA-seq. Our findings underscore GALNT5's novel role in ferroptosis, suggesting its potential as a therapeutic target for PAAD and other malignancies.

Materials and methods

Data collection

Transcriptomic data spanning various cancer types was sourced from the TCGA database (https://portal.gdc.cancer.gov/). Normal tissue RNA-seq transcriptome data, which TCGA lacks, were retrieved from the Genotype-Tissue Expression (GTEx) database (https://gtexportal.org/home/datasets). Additionally, the PAAD data were cross-verified using the Gene Expression Omnibus (GEO) database (GSE62452 and GSE16515). GALNT5 expression profiles of tumor cell lines received validation from the Broad Institute Cancer Cell Line Encyclopedia (CCLE) database (https://portals.broadinstitute.org/ccle/data). Immunohistochemical (IHC) staining data for GALNT5 in PAAD and its normal counterparts were extracted from the Human Protein Atlas (HPA) database (https://www.proteinatlas.org).

Analysis of GALNT5 expressional level and survival outcome

The expression data for this segment was drawn from both the TCGA and GTEx databases. All expression values underwent a log2(x+1) transformation. Differential significance was determined using unpaired Student's t-Tests. Genetic alterations analysis centered on the TCGA dataset. Correlations between GALNT5 and metrics like disease-specific survival (DSS) and progression-free survival (PFS) across various cancer types were determined using univariate Cox analysis and Kaplan-Meier survival analysis via the online platform Aclbi (https://www.aclbi.com/). Clinical parameters for discerning the relationships between GALNT5 expression and tumor stages were sourced from the TCGA database.

Correlation between GALNT5 levels and ferroptosis regulator genes (FRGs)

FRG expression data in a variety of tumors [18] were also extracted from the TCGA dataset. Spearman's correlation analysis was employed to establish the relationship between GALNT5 levels and mean FRG expression. The same analysis method was also used to determine the relationship between GALNT5 levels and each individual FRG across multiple tumors. To gauge the differential FRG expressions between high and low GALNT5 groups, unpaired Student's t-Tests were again utilized. Visualization and data processing were executed using R packages, notably "ggpubr", "corrplot", and "ggplot2".

Immunocyte infiltration analysis

For PAAD patients, the TIMER2.0 algorithm was utilized to estimate the percentages of 10 dis-

tinct immune cell types, as outlined in the quanTIseq algorithm, with guidance from the official TIMER2.0 manual (http://timer.cistrome.org/). The correlations between GALNT5 expression and each type of immune cell infiltration were determined using Spearman's correlation analysis via the online Aclbi tool.

Relationships between GALNT5 levels and ICP genes, tumor mutational burden (TMB), and microsatellite instability (MSI)

Expression data for ICP genes was sourced from the TCGA dataset. The correlation analysis for ICP genes employed the same methodology as that for the FRGs. The relationship between GALNT5 and both TMB and MSI across diverse tumors was elucidated using Spearman's correlation analysis via the online platform, Aclbi.

Protein-protein interaction (PPI) network analysis

Potentially interacting proteins with GALNT5 were identified in STRING (https://string-db.org/). Parameters set included: "minimum required interaction score" at "medium confidence", "meaning of network edges" as "evidence", and "maximum number of interactors to show" capped at 20. The top 20 genes interacting with GALNT5 were visually represented.

Cell lines and transfection

Human PAAD cell lines PANC-1 and sw1990 were procured from the Cell Bank of the Type Culture Collection Committee of the Chinese Academy of Sciences (China). Both PANC-1 and sw1990 cells were cultured in DMEM (Invitrogen, USA) enriched with 10% fetal bovine serum (Invitrogen).

Two mixed siRNA sequences targeting GALNT5 were acquired from Genomeditech (China), and their specific sequences are provided in Supplementary Table 1. Transfection of PANC-1 and sw1990 cells with GALNT5 siRNA (si-GALNT5) or its negative control (si-ctrl) was achieved using the HiPerFect Transfection Reagent (QIAGEN, Germany).

Western blot analysis

Extracted proteins underwent SDS-PAGE gel separation. Western blot tests for human GALNT5 utilized specific antibodies (HPA-008963, Sigma, USA). Human GAPDH was simultaneously assessed using its corresponding antibody (sc-47724, Santa Cruz, USA) as a standard for loading control.

Cell counting kit-8 (CCK-8) assay

Cells, at a seeding density of 5 × 10^3, were allocated to 96-well plates, incubated for 48 hours, and then subjected to analysis using the CCK-8 Kit (Bimake, USA). Absorbance was recorded at 450 nm using an ELx800 microplate reader (BioTek Instruments Inc., USA).

Ethynyl-2-deoxyuridine (EdU) and propidium iodide (PI) incorporation assays

EdU staining was performed using the Click-iT EdU assay (Invitrogen) as per the provided instructions. For the PI procedure, cells were treated with PI (7.5 M, Invitrogen) and incubated in the dark for 10 minutes at 37°C. Both EdU and PI stained cells were visualized under an inverted fluorescence microscope (Olympus, Japan).

Transwell migration and invasion assay

For the transwell migration assay, an 8-μm pore size transwell chamber without Matrigel (3422, Corning, USA) was employed. In contrast, the invasion assay utilized an 8-μm pore size transwell chamber integrated with Matrigel (354480, Corning, USA). Chambers were seeded with 1×10^5 cells in 100 μl of serum-free medium, while 500 μl of medium enriched with 10% FBS served as a chemoattractant in the lower chamber. Post a 24-hour incubation, cells that had not transmigrated were delicately cleared from the upper membrane using cotton swabs. Migrated or invaded cells attached to the lower membrane surface were then stabilized using 4% paraformaldehyde and stained with 1% crystal violet for 15 minutes. The subsequent evaluation of cell invasion was based on counting stained cells from five random microscope fields.

Flow cytometry assays: cell death, lipid reactive oxygen species (ROS), and JC-1

Cell death metrics were derived from staining with SYTOX Green (Invitrogen) followed by flow cytometry analysis. For lipid peroxidation

assessment, cells were subjected to a 30-minute staining at 37°C using 5 μM BODIPY-C11 (Invitrogen), with subsequent flow cytometric examination. Cells showing FITC fluorescence intensities surpassing 99% of the non-stained samples were classified as lipid ROS-positive. The mitochondrial membrane potential was gauged utilizing the MitoProbe™ JC-1 assay (Invitrogen) as per the provided guidelines, with data acquisition via flow cytometry.

Xenograft mouse model

Lentivirus packaging was orchestrated by Genomeditech. PANC-1 cells underwent transfection with either the si-GALNT5 lentivirus or a control variant. Subsequently, 5 × 10^6 PANC-1 cells were introduced subcutaneously to the upper left flank of six-week-old female nude mice (BALB/c; JRDun Biotechnology, China). Each experimental set comprised five mice. Tumor dimensions were recorded every fourth day, with volume calculations following the formula: 0.5 × length × width^2. On day 21 post-tumor cell introduction, euthanasia was administered to all mice, after which the excised tumor specimens were weighed.

RNA-seq analysis

48 hours post-transfection with either si-ctrl or si-GALNT5, PANC-1 cells (from three distinct wells for each group) were harvested. Subsequent total RNA extraction from these cells utilized the TRIzol reagent in line with the manufacturer's guidelines. The extracted RNA then underwent deep sequencing at LC-Bio Co. (China) on the Illumina Novaseq™ 6000 system. Gene Ontology (GO) and KEGG analyses were formulated using the differentially expressed genes (DEGs; with criteria $|\log_2 FC| \geq 1$ and $P < 0.05$) across the two cohorts.

Statistical analysis

All pertinent statistical evaluations were executed utilizing Prism (Version 9.0) software in conjunction with the R language software version R-4.0.3. Data derived from experimental subsets underwent analysis via unpaired Student's t-Tests to ascertain the relevance of observed variances. A two-sided *P*-value less than 0.05 was acknowledged as significant.

Results

Differential expression of GALNT5 in tumor vs. normal tissues

In our endeavor to elucidate differences in GALNT5 expression between tumor and normal samples, we examined GALNT5 mRNA expression data from the TCGA and GTEx databases. Our analysis revealed a marked elevation in GALNT5 mRNA levels across various cancers. These included bladder cancer (BLCA), breast cancer (BRCA), cervical squamous cell carcinoma (CESC), cholangiocarcinoma (CHOL), colon adenocarcinoma (COAD), large B-cell lymphoma (DLBC), esophageal cancer (ESCA), glioblastoma (GBM), kidney clear cell carcinoma (KIRC), kidney papillary cell carcinoma (KIRP), liver hepatocellular carcinoma (LIHC), lung adenocarcinoma (LUAD), ovarian cancer (OV), PAAD, rectal adenocarcinoma (READ), stomach adenocarcinoma (STAD), thyroid cancer (THCA), uterine corpus endometrial carcinoma (UCEC), and uterine carcinosarcoma (UCS), as illustrated in **Figure 1A**. Notably, PAAD showcased the most pronounced expression of GALNT5 among all studied malignancies.

Delving further, we assessed GALNT5 mRNA expression across multiple cancer cell lines via the CCLE database. Herein, GALNT5 expression peaked in lower grade glioma (LGG) cells, followed closely by PAAD cells (Supplementary Figure 1A).

Acknowledging the role of genetic alterations in shaping cancer trajectories, we examined GALNT5's genetic variations across cancers. UCEC exhibited the most frequent GALNT5 alterations (> 7.5%), with missense mutations being predominant (Supplementary Figure 1B).

Prognostic value of GALNT5 across cancer types

To establish a link between GALNT5 expression and patient outcomes, we employed Cox regression and Kaplan-Meier survival analyses. Data from TCGA highlighted that heightened GALNT5 expression correlated with unfavorable DSS outcomes in cancers like BLCA, LGG, and PAAD. Conversely, diminished GALNT5 levels aligned with poor DSS in KIRP and UCS

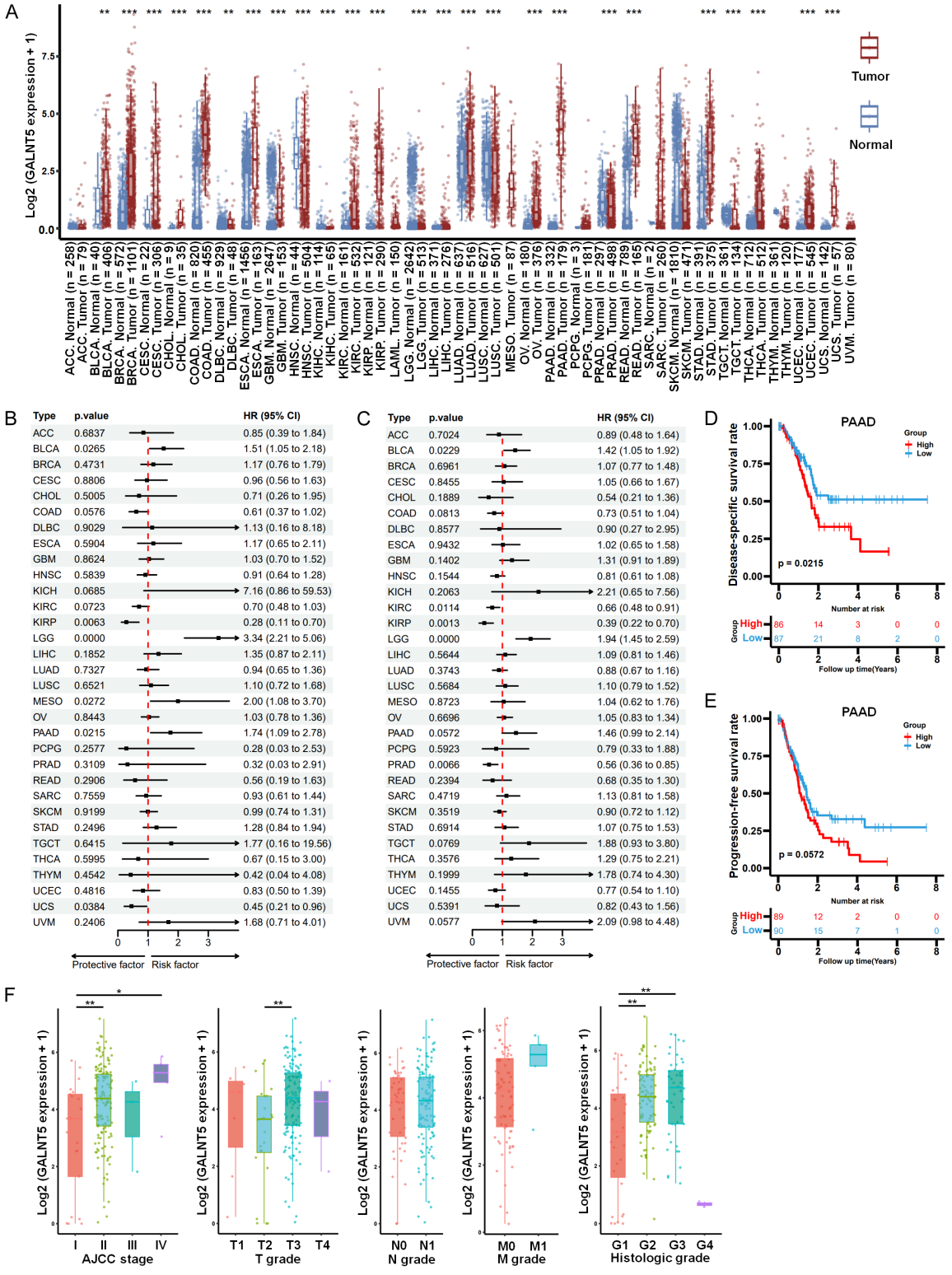

Figure 1. Abnormal expression and clinical significance of GALNT5 in multiple tumors. A. Comparative analysis of GALNT5 expression between normal and tumor tissues across various tumor types, utilizing the TCGA and GTEx databases. B. Association of disease-specific survival (DSS) with GALNT5 expression across multiple tumors. C. Relationship between GALNT5 expression and progression-free survival (PFS) in various tumors. D. Kaplan-Meier survival curves depicting DSS with respect to GALNT5 expression in PAAD patients. E. Kaplan-Meier survival curves showing PFS in relation to GALNT5 expression in PAAD patients. F. GALNT5 expression levels across different AJCC stages and histologic grades within PAAD patients. *$P < 0.05$; **$P < 0.01$; ***$P < 0.001$.

(**Figure 1B**, **1D** and Supplementary Figure 2A). Moreover, elevated GALNT5 levels were negatively associated with PFS in BLCA and LGG but showed a positive correlation in KIRC, KIRP, and PRAD (**Figure 1C** and Supplementary Figure 2B). Notably, a near-significant trend was observed with PAAD patients showcasing high GALNT5 levels and poor PFS (*P* value = 0.0572) (**Figure 1E**).

Considering GALNT5's aberrant expression and its prognostic implications in PAAD, further investigations were conducted. We noted that GALNT5 levels in AJCC stage I and histologic grade G1 cases were subdued relative to other stages (**Figure 1F**). Contrarily, RAB22A overexpression in HCC was closely tethered to clinicopathological attributes. Subsequent assessments of the GEO database (GSE62452, GSE16515) reiterated GALNT5's overexpression in PAAD relative to standard samples (Supplementary Figure 3A, 3B). This overexpression was further confirmed through IHC staining from the HPA database, underscoring GALNT5's heightened presence in PAAD tissues compared to normal pancreatic tissues (Supplementary Figure 3C, 3D).

Potential role of GALNT5 in ferroptosis

To ascertain the potential role of GALNT5 in ferroptosis, we examined the correlation between GALNT5 and a gene set of 24 FRGs [18]. As shown in **Figure 2A** and Supplementary Figure 4, GALNT5 was significantly correlated with FRGs in 26 out of 33 cancer types. Additionally, GALNT5's expression was found to significantly correlate with the expressions of numerous FRGs across diverse cancers (**Figure 2B**).

Within the array of analyzed cancers, the most robust correlation between GALNT5 and FRGs was observed in PAAD, characterized by an R value of 0.65 (**Figure 2C**). Among the 24 FRGs, 18 were overexpressed in the GALNT5 high expression group in PAAD, including genes such as ATP5MC3, CARS1, CDKN1A, and others, whereas only GSL2 was upregulated in the GALNT5 low expression group (**Figure 2D**). Similarly, GALNT5's expression was significantly positively correlated with 18 FRGs (Supplementary Figure 5), many of which act as suppressors of ferroptosis, such as CDKN1A, FANCD2, NFE2L2, and SLC7A11 [19-22]. These findings support the notion that GALNT5 may serve as a potential regulator of ferroptosis, particularly in PAAD.

Correlations of GALNT5 expression with immune cell infiltration and ICP

Recognizing ferroptosis's significant function in immune regulation, we explored GALNT5's potential effect on immune infiltration and ICP. **Figure 3A** illustrates that GALNT5 expression is significantly correlated with various immune cell infiltrations in the majority of cancer types. Notably, the expression was broadly and positively correlated with M1 macrophages in 22 cancers, regulatory T cells in 18, neutrophils in 17, and M2 macrophages in 16. Since ICP inhibitors are among the primary treatments for many cancers, we probed the relationships between GALNT5 levels and 47 common ICP genes [23], uncovering that the relationship with ICP genes differed across cancer types. GALNT5 expression was positively associated with most ICP genes in numerous cancers, including BLCA, LGG, LIHC, and THCA (Supplementary Figure 6).

In addition, in PAAD, GALNT5 level correlated positively with M1 macrophage and neutrophil infiltration and negatively with the infiltration of M2 macrophages, monocytes, NK cells, CD8+ T cells, regulatory T cells, and dendritic cells (**Figure 3B**). Moreover, 10 ICP genes were upregulated and 10 were downregulated in the GALNT5 high expression group of PAAD (**Figure 3C**). These outcomes hint at GALNT5's potential role in disrupting the immune microenvironment (IME) balance in cancers.

TMB and MSI, two emerging biomarkers linked with immunotherapy response [24], were further analyzed in correlation with GALNT5 expression across cancers. The analysis revealed that GALNT5 expression had a positive correlation with TMB in THYM, PAAD, ESCA, LGG, COAD, and STAD and a negative correlation in PRAD, LUAD, BRCA, LIHC, UCEC, and CESC (Supplementary Figure 7A, 7B; Supplementary Table 2). Additionally, GALNT5 expression demonstrated a positive correlation with MSI in COAD, READ, testicular germ cell tumor (TGCT), and ESCA and a negative correlation in UCEC, PRAD, CESC, and LUAD (Supplementary Figure 7C, 7D; Supplementary Table 2).

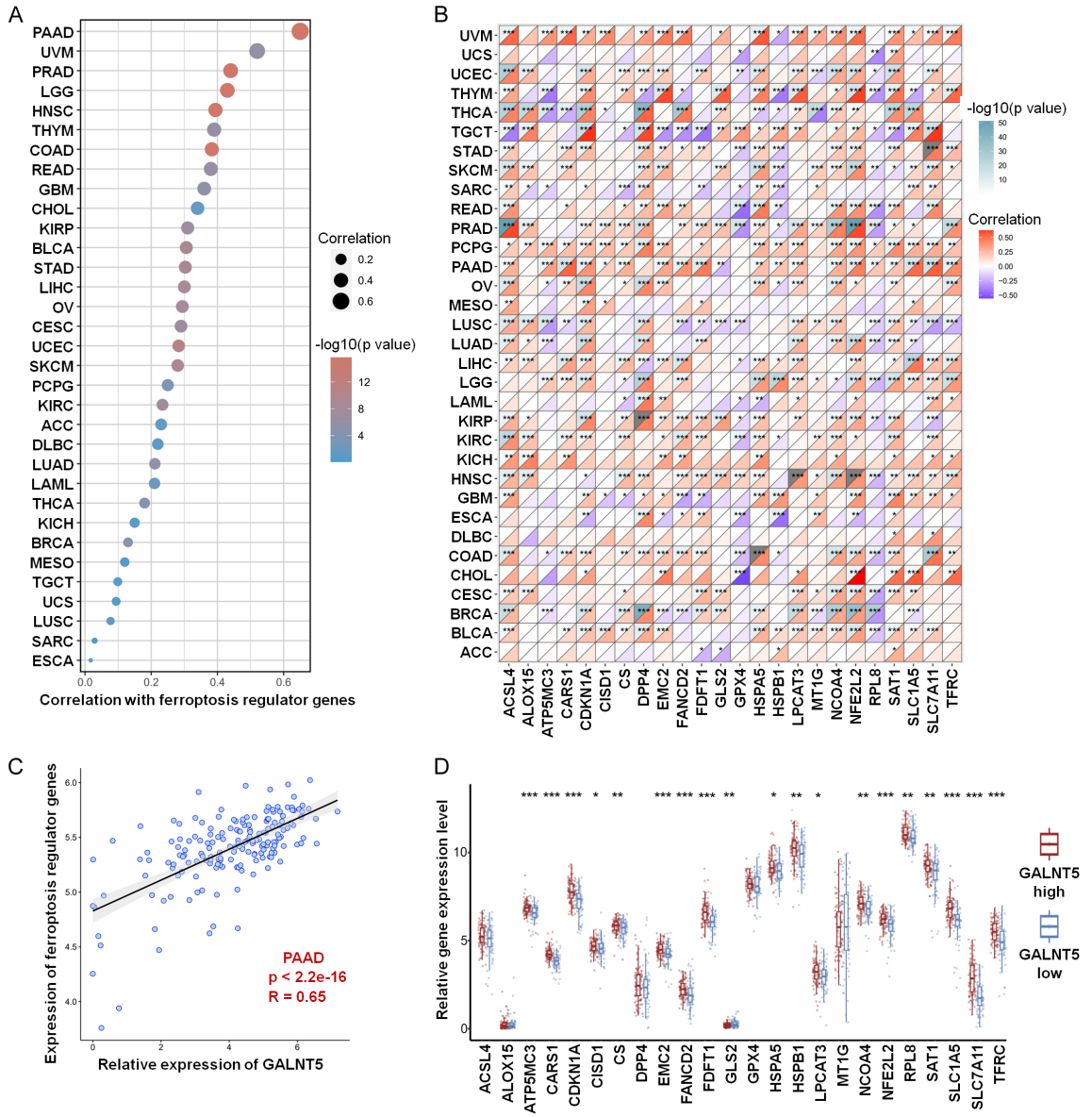

Figure 2. Analysis of the correlation between GALNT5 expression and ferroptosis. A. Correlation of GALNT5 expression levels with the mean expression of ferroptosis-related genes (FRGs) in multiple tumors. B. Relationship between GALNT5 expression and individual FRG expression across various tumors. C. Association of GALNT5 expression with the mean expression of FRGs in PAAD. D. Differential expression of FRGs in high and low GALNT5 expression groups among PAAD patients. *$P < 0.05$; **$P < 0.01$; ***$P < 0.001$.

Knockdown of GALNT5 expression inhibits proliferation, migration and invasion in PAAD cells

To elucidate the role of GALNT5 in PAAD cells, we initially examined the expression of GALNT5 across several cell lines. Notably, GALNT5 was found to be overexpressed in all four PAAD cell lines when compared with the pancreatic ductal epithelial cell line (**Figure 4A**). Given this pronounced expression, we chose PANC-1 and sw1990 for further analysis, employing transfection with siGALNT5. The inhibition of GALNT5 was subsequently validated via Western blotting (**Figure 4B**). The CCK8 assay results revealed a significant inhibition of PANC-1 and sw1990 cell proliferation following the transfection with either si-GALNT5-1 or si-GALNT5-2 (**Figure 4C**). As EdU incorporation is indicative of DNA synthesis and cell proliferation activity, the suppression of GALNT5 further resulted in

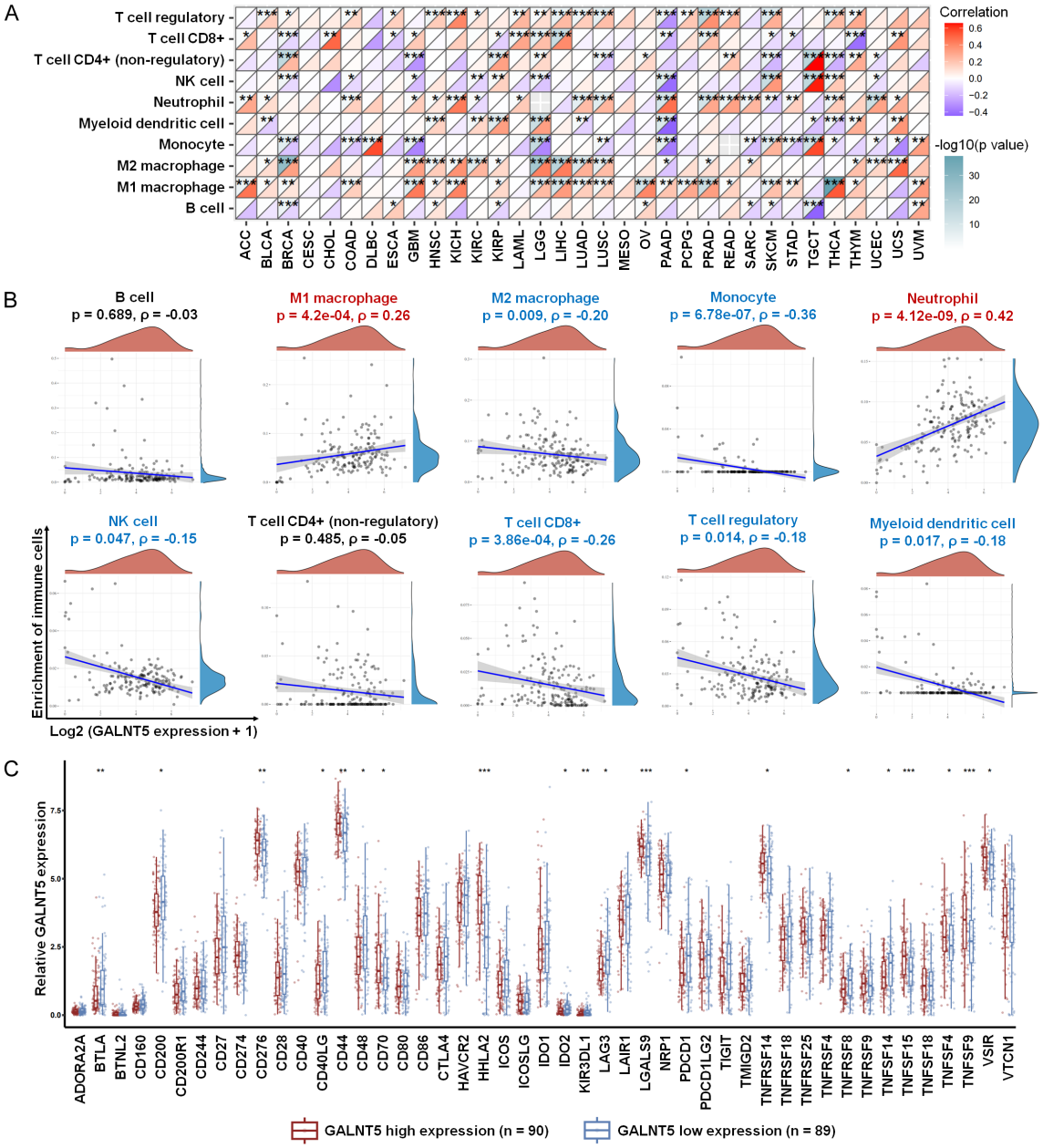

Figure 3. Exploration of the relationship between GALNT5 and the immune microenvironment in PAAD and other tumors. A. Correlation analysis between GALNT5 expression and the infiltration of immunocytes across multiple cancer types. B. Investigation of the relationship between GALNT5 expression and infiltration of 10 distinct immune cell subtypes. C. Differences in the expression of immune checkpoint (ICP) genes between the high and low GALNT5 expression groups in PAAD patients. *$P < 0.05$; **$P < 0.01$; ***$P < 0.001$.

a significant reduction in EdU-positive cells in both cell lines (**Figure 4D**). Moreover, transwell assays demonstrated decreased migration in PANC-1 and sw1990 cells after either si-GALNT5-1 or si-GALNT5-2 transfection (**Figure 4E**). The use of Matrigel-coated transwell chambers revealed that the invasion capability was also reduced following GALNT5 inhibition (**Figure 4F**). Collectively, these findings imply that GALNT5 may play an activating role in the proliferation, migration, and invasion of PAAD cells.

Knockdown of GALNT5 expression promotes ferroptosis in PAAD cells

Given the previously identified close connection between GALNT5 and ferroptosis in pan-

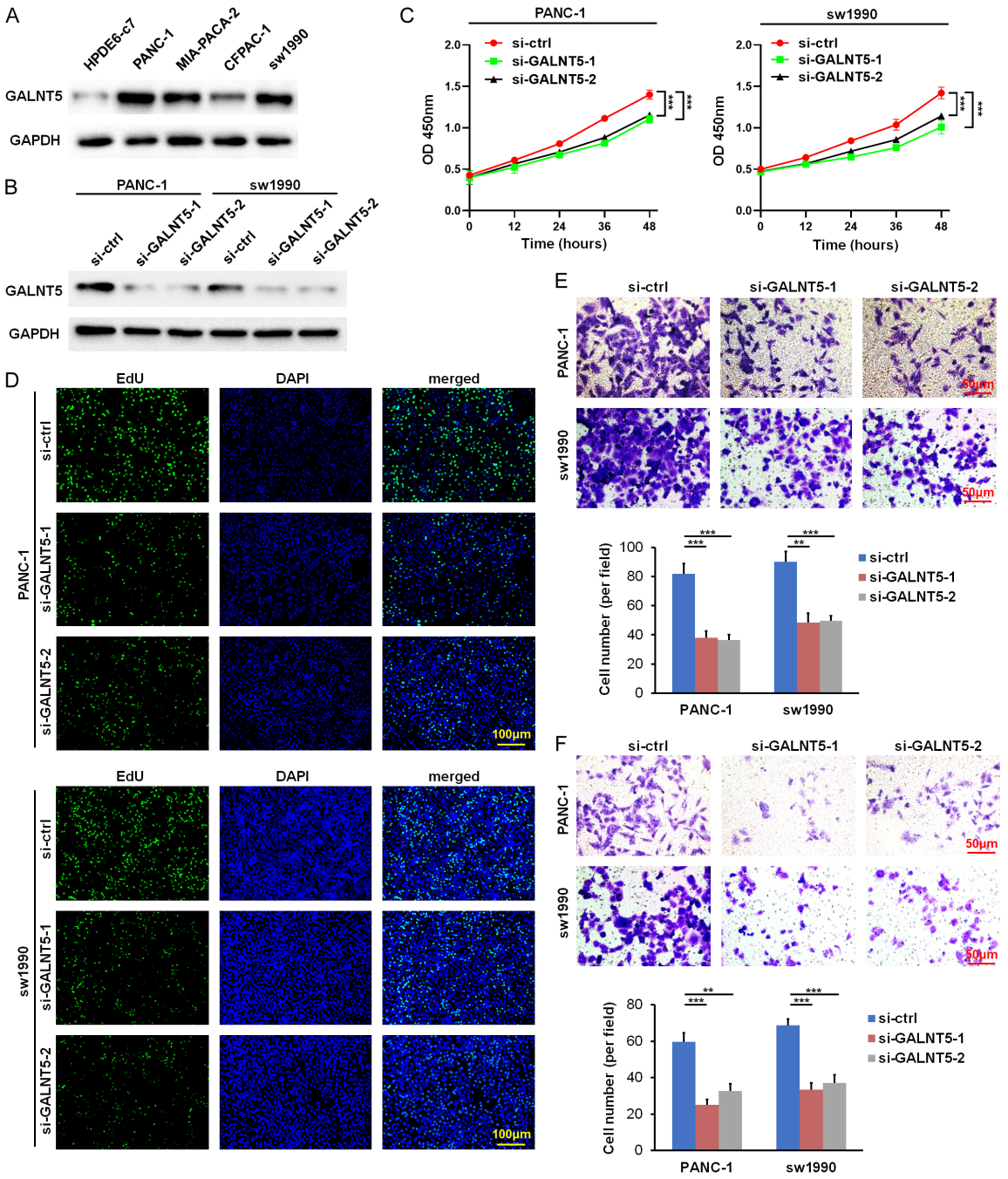

Figure 4. Inhibition of GALNT5 expression suppresses PAAD cell proliferation, migration and invasion. A. Western blot analysis of GALNT5 in a normal pancreatic ductal epithelial cell line (HPDE6-c7) and four PAAD cell lines (PANC-1, MIA-PACA-2, CFPAC-1 and sw1990). B. GALNT5 expression in PANC-1 and sw1990 cells transfected with si-ctrl, si-GALNT5-1 or si-GALNT5-2, examined through Western blot assay. C. CCK8 assay for PANC-1 and sw1990 cells following transfection with si-ctrl or si-GALNT5-1/2. D. EdU staining to detect DNA replication in PANC-1 and sw1990 cells after GALNT5 knockdown. E. Evaluation of migration capacity in PANC-1 and sw1990 cells post-transfection with si-ctrl or si-GALNT5-1/2, using a transwell assay. F. Assessment of invasion capacity in PANC-1 and sw1990 cells post-GALNT5 knockdown, employing the transwell assay with Matrigel. $^{**}P < 0.01$; $^{***}P < 0.001$.

cancer analyses, we further investigated GALNT5's role in the regulation of ferroptosis by detecting total cell death in PANC-1 and sw1990 cells via PI staining. The outcomes indicated that transfection with either si-GALNT5-1 or si-GALNT5-2 notably accelerated cell death in both cell lines (**Figure 5A**). To ascertain the type of cell death induced by

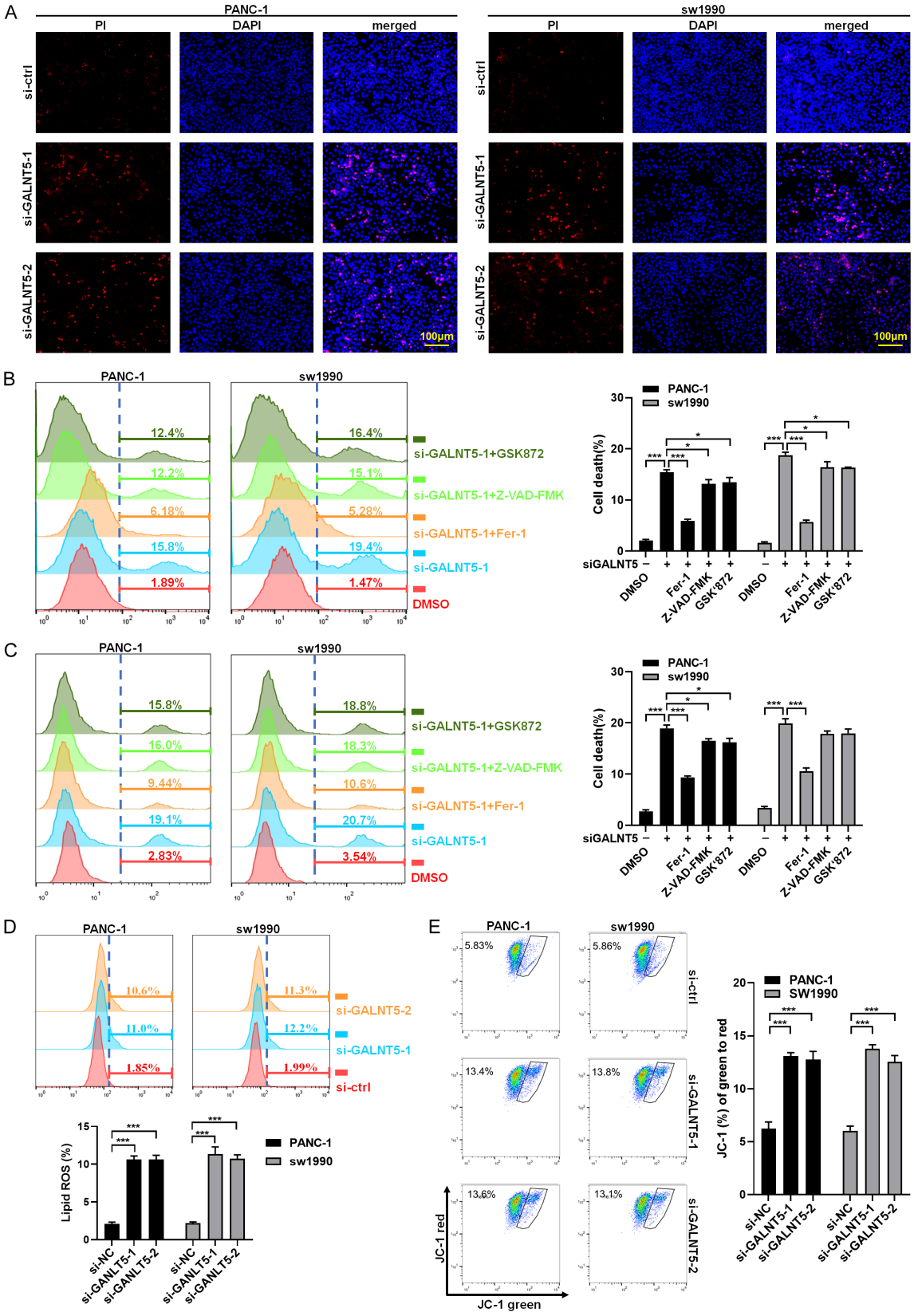

Figure 5. GALNT5 inhibition activates ferroptosis in PAAD cells. A. PI staining to observe cell death in PANC-1 and sw1990 cells following transfection with si-ctrl or si-GALNT5-1/2. B. Treatment of PANC-1 and sw1990 cells trans-

fected with si-GALNT5-1 with 1 μM Fer-1, 20 μM of the pan-caspase inhibitor Z-VAD-FMK, or 10 μM of the RIPK3 inhibitor GSK872 for 30 h, followed by SYTOX Green staining and flow cytometry to measure cell death. C. Cell death measurement in PANC-1 and sw1990 cells transfected with si-GALNT5-2 and treated with Fer-1, Z-VAD-FMK, or GSK872. D. Lipid ROS production assessment in PANC-1 and sw1990 cells post-transfection with si-ctrl or si-GALNT5-1/2, utilizing BODIPY-C11 staining and flow cytometry. E. Mitochondrial membrane potential levels in PANC-1 and sw1990 cells following GALNT5 inhibition, measured with JC-1 staining and flow cytometry. *$P < 0.05$; ***$P < 0.001$.

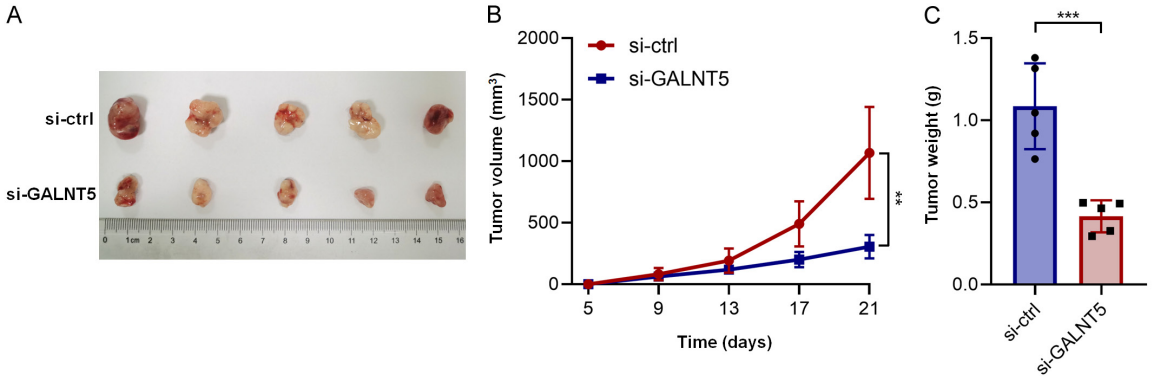

Figure 6. GALNT5 inhibition suppresses tumor growth of PAAD in vivo. A. Transplantation of PANC-1 cells transduced with si-GALNT5 lentivirus or control lentivirus into nude mice. After 21 days, the tumors were extracted and measured. B. Regular measurement of tumor volumes over the 21-day period. C. Weights of the harvested tumors in both groups. **$P < 0.01$; ***$P < 0.001$.

GALNT5 inhibition, cells were preincubated with specific inhibitors, including Fer-1 for ferroptosis, Z-VAD-FMK for necroptosis, and GSK872 for apoptosis, following si-GALNT5 transfection. Examination of cell death through flow cytometry revealed that Fer-1 significantly reversed si-GALNT5-induced cell death, whereas Z-VAD-FMK and GSK872 had limited effects (**Figure 5B**, **5C**). Lipid ROS detection further substantiated that either si-GALNT5-1 or si-GALNT5-2 markedly elevated lipid ROS in comparison with si-ctrl in both cell lines (**Figure 5D**). Additionally, JC-1 examination demonstrated an increased mitochondrial membrane potential after GALNT5 suppression, as evidenced by the enhanced green-to-red fluorescence ratio (**Figure 5E**). These results collectively highlight GALNT5's function as a suppressor of ferroptosis.

Inhibition of GALNT5 suppresses tumor growth of PAAD in vivo

GALNT5, known to promote cell proliferation and migration and inhibit ferroptosis in PAAD cells in vitro, prompted an investigation of its possible role in vivo. A subcutaneous tumor model was created using nude mice, injected with PANC-1 cells transfected with either si-GALNT5 lentivirus or control lentivirus. After a period of 21 days, both tumor volume and weight had markedly decreased in the GALNT5 knockdown group compared to the control group (**Figure 6A-C**), indicating that the inhibition of GALNT5 can suppress the tumor growth of PAAD in vivo.

Exploring the possible downstream of GALNT5 in PAAD cells

The potential mechanism of GALNT5 in cancer was probed by analyzing the interaction network of GALNT5, supported by data from the STRING website. **Figure 7A** illustrates that the most related genes are part of the mucin (MUC) family, the substrates for O-glycosylation by GALNTs. Further examination of other potential molecular mechanisms involved conducting RNA-seq on PANC-1 cells transfected with either si-ctrl or si-GALNT5. A total of 187 genes were significantly upregulated (fold change > 2, P < 0.05), and 245 genes were downregulated after GALNT5 inhibition (**Figure 7B**; Supplementary Table 3). Gene Ontology (GO) and Kyoto Encyclopedia of Genes and Genomes (KEGG) pathway analyses revealed that GALNT5 expression is associated with numerous immune- and inflammation-related

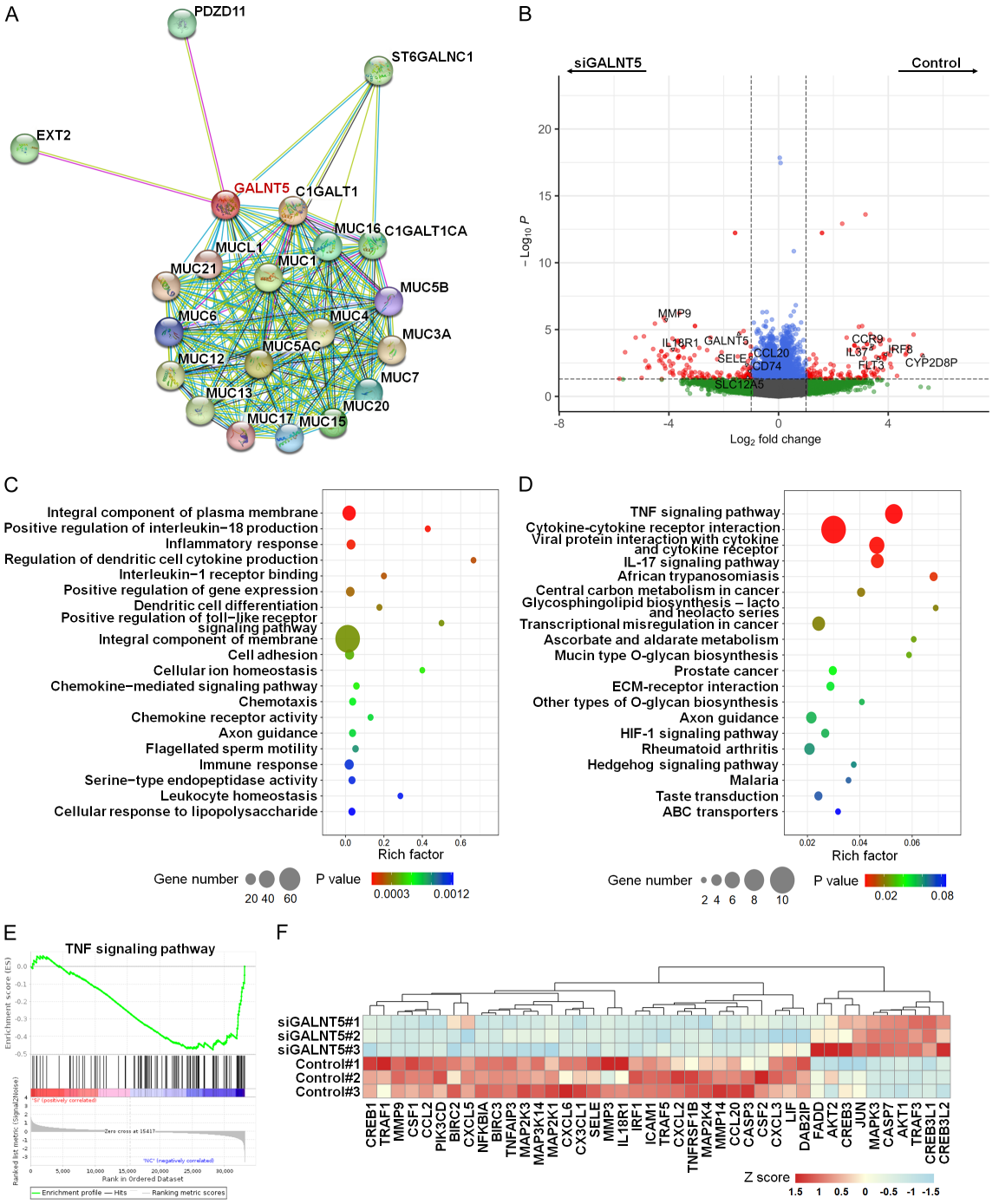

Figure 7. Examination of potential downstream of GALNT5 in PAAD cells. A. Interaction network comprising 20 GALNT5-associated proteins, as derived from STRING. B. RNA-seq of PANC-1 cells conducted post-transfection with either si-ctrl or si-GALNT5, with differentially expressed genes (DEGs) depicted in a volcano plot. C. Gene Ontology (GO) pathway analysis of the DEGs between the si-ctrl and si-GALNT5 groups. D. Kyoto Encyclopedia of Genes and Genomes (KEGG) pathway analysis of the DEGs. E. Gene Set Enrichment Analysis (GSEA) of changes in the TNF signaling pathway following GALNT5 inhibition. F. Heatmap illustrating the altered genes ($P < 0.05$) in the TNF signaling pathway after GALNT5 inhibition.

pathways, including the inflammatory response, dendritic cell cytokine production regulation, chemotaxis, and immune response pathways (**Figure 7C**). KEGG pathway analyses revealed

that mucin type O-glycan biosynthesis pathway was regulated by GALNT5, which is consistent with the major reported role of GALNTs [25]. The outcomes further highlighted the alteration of TNF signaling pathway after GALNT5 inhibition (**Figure 7D**). In addition, GSEA analysis revealed that TNF signaling pathway was suppressed in GALTN5 inhibition cells (**Figure 7E**). As shown in **Figure 7F**, out of the 111 genes in the TNF signaling pathway, 42 were altered ($P < 0.05$) after GALNT5 inhibition, including genes like CSF2, CCL20, MMP9, and CXCL5. These findings suggest GALNT5's involvement in immune and inflammation regulation, with the TNF signaling pathway possibly being a downstream effect.

Discussion

Protein glycosylation, a common post-translational modification controlled by enzymes, mainly includes two categories: N-glycosylation and O-glycosylation [26]. Mucin-type O-glycosylation, synthesized by GALNTs and abundant in mucins, represents the most common and diverse type [27, 28]. Mucins, comprising a class of membrane-bound and secreted glycoproteins, broadly influence tumor progression [28]. Certain mucins are widely utilized as tumor markers in clinical practice, for instance, MUC16 (CA125) for ovarian cancer, MUC1 (CA153) for breast cancer, and CA199 for pancreatic adenocarcinoma (PAAD) [29-31]. Furthermore, alterations in the structure and quantity of mucin-type O-glycans yield tumor-specific glycan structures in tumor cells, like Tn and T antigens, which are intricately linked to tumor exacerbation [26]. Thus, the aberrant expression of GALNTs directly impacts the synthesis of O-glycans, demonstrating potential for controlling malignant phenotypes. Previous studies have reported GALNT1 overexpression as promoting metastasis and predicting poor prognosis in gastric cancer and osteosarcoma [5, 32], with GALNT2 supporting tumor formation in non-small cell lung cancer and glioma [10, 33], and GALNT3 maintaining the self-renewal of cancer stem cells in PAAD [34].

The activation of ferroptosis is increasingly viewed as a potent strategy for cancer therapy, with considerable focus on amplifying tumor cell sensitivity to this form of cell death [35]. There is burgeoning evidence pointing to the role of mucin-type O-glycans in ferroptosis regulation. Wang et al. [36] illustrated that MUC1 counters ferroptosis through the GSK3β/Keap1-Nrf2-GPX4 pathway in cases of acute lung injury. MUC16 mutations have been linked to ferroptosis-related prognostic models in esophageal squamous cell carcinoma [37]. Tian et al. [38] flagged GALNT9 as a ferroptosis-associated gene in glioblastoma, and evidence suggests that GALNT14 might inhibit ferroptosis via the EGFR/mTOR pathway [39]. Notably, GALNT5 emerged as one of the genes most downregulated during ferroptosis [14], yet its specific role in this process remains unclear.

The function of GALNT5 has been probed across multiple tumor types. Detarya et al. [12, 13] postulated that GALNT5 underpins the genesis and progression of cholangiocarcinoma, chiefly through AKT/ERK and EGFR pathways. Stiegelbauer et al. [40] found that GALNT5 augments the motility of colorectal cancer cells and is modulated by miR-196b-5p. An overexpression of GALNT5 was documented in hepatoblastoma [41], and it has been linked to unfavorable outcomes in hepatocellular carcinoma [11]. However, the expression landscape of GALNT5 in PAAD is not consistent. Yan et al. [42] observed its upregulation in PAAD, contrasted by Caffrey et al. [43] who noted MUC1-driven downregulation of GALNT5 in the same context. Despite these observations, the exact function of GALNT5 in PAAD cells remains largely unexplored. Our current investigation reveals an upregulation of GALNT5 across 18 tumor types relative to normal tissue, with PAAD exhibiting the most pronounced GALNT5 expression in tumors and ranking second in tumor cell lines. Further, using the TCGA database, GALNT5 was pinpointed as a potential prognostic marker. An overarching pan-cancer analysis also denoted a significant association between GALNT5 expression and ferroptosis-related genes across various cancers. Consequently, we delved into the potential role of GALNT5 in PAAD cells. Our findings underscored that GALNT5 knockdown suppressed both the growth and migration of PAAD cells. This study also unveils, for the first time, that GALNT5 inhibition can catalyze ferroptosis. In vivo experiments using a mouse model further endorsed GALNT5's oncogenic character.

Ferroptosis has been found to play crucial roles in the regulation of tumor immunity and response to immunotherapy [15, 16]. Many solid tumors, termed “cold tumors”, are characterized by a scarcity of immune cells, making them difficult for drugs to penetrate [44, 45]. Ferroptotic tumor cells frequently release damage-associated molecular patterns (DAMPs) or lipid metabolites, modulating the cellular immune response by affecting macrophage-mediated phagocytosis and immune cell function [46, 47]. Therefore, the application of ferroptosis-inducing agents may increase the immunogenicity of “cold tumors”, transforming them into more immunotherapy-sensitive “warm tumors” [15]. Moreover, CD8+ T cells activated by immune checkpoint inhibitors can release interferon γ, subsequently inducing cancer cell ferroptosis by suppressing the expression of SLC3A2 and SLC7A11 [48]. Consistent with these concepts, there has been a growing body of research on the use of combined immunotherapy with ferroptosis inducers for tumor treatment. Liu et al. [49] explored a ferroptosis-inducing combined immunotherapy drug, Fe3O4-siPD-L1@M-BV2, to target immune-resistant brain glioblastoma multiforme (GBM). A combination therapy involving the ferroptosis-inducing natural compound withaferin A and α-PD-1 demonstrated a marked improvement in survival rates for mice afflicted with liver tumors [50]. Similarly, a synergistic approach combining nanoparticle-induced ferroptosis with PD-L1 blockade effectively suppressed both the growth of melanoma and lung metastasis in breast cancer [51].

The upregulation of glycosylation in membrane-bound mucins has been observed in numerous cancers, possibly shielding cancer cells from immune detection [52]. Tn (GalNAc-Ser/Thr) and STn (NeuAcα2-6GalNAc-Ser/Thr) are identified as cancer-associated truncated glycans expressed in many tumors. Previous research has shown that inhibiting Tn and STn can significantly enhance sensitivity to NK cell-mediated cellular-cytotoxicity and cytotoxic T lymphocyte-mediated killing [51]. As enzymes of mucin-type O-glycosylation, GALNTs have also been found to function in tumor immunity. GALNT3, GALNT7, and GALNT16 are identified as potential indicators for immunotherapy [53-55], while overexpression of GALNT14 correlates with reduced immunogenic cell death and the progression of malignancies like osteosarcoma [56]. Considering the roles of ferroptosis and O-glycosylation in tumor immunity, we explored the potential correlations of GALNT5 expression with immune infiltration and immunotherapy. We discovered that GALNT5 expression was positively correlated with the infiltration of regulatory T cells, immune suppressors, and M2 macrophages, as well as several ICP genes across various tumors. These findings propose GALNT5 as a potential regulator of tumor immunity that may be associated with tumor immunotherapy.

The mechanism underlying GALNT5’s function remains largely undefined. We conducted RNA-seq following GALNT5 inhibition in a PAAD cell line, identifying fluctuations in the expressions of various inflammation-related cytokines and receptors such as CXCL6, TNFRSF4, CCL20, CCR9, and IL37. Pathway analysis further revealed alterations in many immune-related pathways, including changes in several interleukin (IL)-related pathways such as the positive regulation of IL18 production, IL1 receptor binding, and the IL17 signaling pathway. Additionally, KEGG analysis indicated that the TNF signaling pathway was the most significantly affected. GSEA analysis also highlighted the inhibition of the TNF signaling pathway following GALNT5 knockdown. Given that the TNF pathway plays a major role in inflammation and immune regulation [57, 58], and is a key player in ferroptosis [59, 60]. Thus, we consider that TNF signaling pathway may be a downstream mediator of GALNT5, orchestrating the changes in ferroptosis and immunity induced by GALNT5.

Our findings underscore the upregulation of GALNT5 in PAAD and several other tumors, indicative of an adverse prognosis for patients. Subsequent studies have recognized GALNT5 as a novel suppressor of ferroptosis, playing a part in the regulation of the immune microenvironment (IME). Given the essential roles of ferroptosis in eradicating tumor cells and enhancing the efficacy of anti-tumor immunotherapy [48], it is proposed that GALNT5 may serve as a prognostic predictor. Moreover, therapies targeting GALNT5 could heighten the responsiveness to immunotherapy in PAAD and other tumors. Nevertheless, future investigations are imperative. Firstly, the associations

between GALNT5 expression and the effectiveness of immunotherapy or chemotherapy remain undetected in clinical samples. Secondly, supplementary experimental studies are warranted to elucidate the specific downstream mechanism of GALNT5. Thirdly, examination of the potential collaboration between immune therapy and GALNT5 inhibition is necessitated.

Conclusion

The present study reveals that GALNT5 is augmented and correlates with patient prognosis in multiple tumors, with particular prominence in PAAD. The expression of GALNT5 is significantly associated with ferroptosis, immune infiltration, and ICP genes across various cancers. Additionally, GALNT5 inhibition markedly curtails the proliferation and migration of PAAD cells, while fostering their ferroptosis. RNA-seq analysis unveils extensive alterations in inflammation and immune-related pathways subsequent to GALNT5 inhibition, and identifies the TNF signaling pathway as a probable downstream target of GALNT5. Collectively, these findings assert that GALNT5 is an innovative regulator of ferroptosis, and may be leveraged as a prognostic marker for survival and immunotherapy in the realm of cancer treatment.

Acknowledgements

This work was supported by the National Natural Science Foundation of China (81874180 and 81872505).

Disclosure of conflict of interest

None.

Address correspondence to: Zhipeng Wu and Ting Wang, Department of Orthopedic Oncology, Shanghai Changzheng Hospital, Naval Medical University, Shanghai, China. E-mail: eaglewzp@163.com (ZPW); wangt_boneleven@163.com (TW); Zhenhua Wang, Department of Laboratory Medicine, Shanghai Changzheng Hospital, Naval Medical University, Shanghai, China. E-mail: zhenhua_wang0517@163.com

References

[1] GBD 2019 Cancer Risk Factors Collaborators. The global burden of cancer attributable to risk factors, 2010-19: a systematic analysis for the Global Burden of Disease Study 2019. Lancet 2022; 400: 563-591.

[2] Zhang R, Peng Y, Gao Z, Qian J, Yang K, Wang X, Lu W, Zhu Y, Qiu D, Jin T, Wang G, He J and Liu N. Oncogenic role and drug sensitivity of ETV4 in human tumors: a pan-cancer analysis. Front Oncol 2023; 13: 1121258.

[3] Siegel RL, Miller KD, Wagle NS and Jemal A. Cancer statistics, 2023. CA Cancer J Clin 2023; 73: 17-48.

[4] Pinho SS and Reis CA. Glycosylation in cancer: mechanisms and clinical implications. Nat Rev Cancer 2015; 15: 540-555.

[5] Zhang J, Wang H, Wu J, Yuan C, Chen S, Liu S, Huo M, Zhang C and He Y. GALNT1 enhances malignant phenotype of gastric cancer via modulating CD44 glycosylation to activate the Wnt/beta-catenin signaling pathway. Int J Biol Sci 2022; 18: 6068-6083.

[6] Ju T, Otto VI and Cummings RD. The Tn antigen-structural simplicity and biological complexity. Angew Chem Int Ed Engl 2011; 50: 1770-1791.

[7] Bard F and Chia J. Cracking the glycome encoder: signaling, trafficking, and glycosylation. Trends Cell Biol 2016; 26: 379-388.

[8] Chia J, Tham KM, Gill DJ, Bard-Chapeau EA and Bard FA. ERK8 is a negative regulator of O-GalNAc glycosylation and cell migration. Elife 2014; 3: e01828.

[9] Festari MF, da Costa V, Rodriguez-Zraquia SA, Costa M, Landeira M, Lores P, Solari-Saquieres P, Kramer MG and Freire T. The tumor-associated Tn antigen fosters lung metastasis and recruitment of regulatory T cells in triple negative breast cancer. Glycobiology 2022; 32: 366-379.

[10] Liu Y, Chen P, Xu L, Wang B, Zhang S and Wang X. GALNT2 sustains glioma stem cells by promoting CD44 expression. Aging (Albany NY) 2023; 15: 2208-2220.

[11] Deng Z, Wang J, Xu B, Jin Z, Wu G, Zeng J, Peng M, Guo Y and Wen Z. Mining TCGA database for tumor microenvironment-related genes of prognostic value in hepatocellular carcinoma. Biomed Res Int 2019; 2019: 2408348.

[12] Detarya M, Sawanyawisuth K, Aphivatanasiri C, Chuangchaiya S, Saranaruk P, Sukprasert L, Silsirivanit A, Araki N, Wongkham S and Wongkham C. The O-GalNAcylating enzyme GALNT5 mediates carcinogenesis and progression of cholangiocarcinoma via activation of AKT/ERK signaling. Glycobiology 2020; 30: 312-324.

[13] Detarya M, Lert-Itthiporn W, Mahalapbutr P, Klaewkla M, Sorin S, Sawanyawisuth K, Silsirivanit A, Seubwai W, Wongkham C, Araki N and Wongkham S. Emerging roles of GALNT5 on promoting EGFR activation in cholangiocar-

cinoma: a mechanistic insight. Am J Cancer Res 2022; 12: 4140-4159.
[14] Riccio G, Nuzzo G, Zazo G, Coppola D, Senese G, Romano L, Costantini M, Ruocco N, Bertolino M, Fontana A, Ianora A, Verde C, Giordano D and Lauritano C. Bioactivity screening of antarctic sponges reveals anticancer activity and potential cell death via ferroptosis by mycalols. Mar Drugs 2021; 19: 459.
[15] Zheng S and Guan XY. Ferroptosis: promising approach for cancer and cancer immunotherapy. Cancer Lett 2023; 561: 216152.
[16] Gu X, Liu Y, Dai X, Yang YG and Zhang X. Deciphering the potential roles of ferroptosis in regulating tumor immunity and tumor immunotherapy. Front Immunol 2023; 14: 1137107.
[17] Yao F, Zhan Y, Pu Z, Lu Y, Chen J, Deng J, Wu Z, Chen B, Chen J, Tian K, Ni Y and Mou L. LncRNAs target ferroptosis-related genes and impair activation of CD4(+) T cell in gastric cancer. Front Cell Dev Biol 2021; 9: 797339.
[18] Liu Z, Zhao Q, Zuo ZX, Yuan SQ, Yu K, Zhang Q, Zhang X, Sheng H, Ju HQ, Cheng H, Wang F, Xu RH and Liu ZX. Systematic analysis of the aberrances and functional implications of ferroptosis in cancer. iScience 2020; 23: 101302.
[19] Forcina GC, Pope L, Murray M, Dong W, Abu-Remaileh M, Bertozzi CR and Dixon SJ. Ferroptosis regulation by the NGLY1/NFE2L1 pathway. Proc Natl Acad Sci U S A 2022; 119: e2118646119.
[20] Kang R, Kroemer G and Tang D. The tumor suppressor protein p53 and the ferroptosis network. Free Radic Biol Med 2019; 133: 162-168.
[21] Li X and Liu J. FANCD2 inhibits ferroptosis by regulating the JAK2/STAT3 pathway in osteosarcoma. BMC Cancer 2023; 23: 179.
[22] Shen L, Zhang J, Zheng Z, Yang F, Liu S, Wu Y, Chen Y, Xu T, Mao S, Yan Y, Li W, Zhang W and Yao X. PHGDH inhibits ferroptosis and promotes malignant progression by upregulating SLC7A11 in bladder cancer. Int J Biol Sci 2022; 18: 5459-5474.
[23] Guo Y, Heng Y, Chen H, Huang Q, Wu C, Tao L and Zhou L. Prognostic values of METTL3 and its roles in tumor immune microenvironment in pan-cancer. J Clin Med 2022; 12: 155.
[24] Wang Y, Guo Y, Song Y, Zou W, Zhang J, Yi Q, Xiao Y, Peng J, Li Y and Yao L. A pan-cancer analysis of the expression and molecular mechanism of DHX9 in human cancers. Front Pharmacol 2023; 14: 1153067.
[25] Ogawa M, Tanaka A, Namba K, Shia J, Wang JY and Roehrl MH. Early-stage loss of galnt6 predicts poor clinical outcome in colorectal cancer. Front Oncol 2022; 12: 802548.
[26] Zhou F, Ma J, Zhu Y, Wang T, Yang Y, Sun Y, Chen Y, Song H, Huo X and Zhang J. The role and potential mechanism of O-Glycosylation in gastrointestinal tumors. Pharmacol Res 2022; 184: 106420.
[27] Bennett EP, Mandel U, Clausen H, Gerken TA, Fritz TA and Tabak LA. Control of mucin-type O-glycosylation: a classification of the polypeptide GalNAc-transferase gene family. Glycobiology 2012; 22: 736-756.
[28] Zhang Y, Sun L, Lei C, Li W, Han J, Zhang J and Zhang Y. A sweet warning: mucin-type O-glycans in cancer. Cells 2022; 11: 3666.
[29] Iwamura T and Katsuki T. Kinetics of carcinoembryonic antigen and carbohydrate antigen 19-9 production in a human pancreatic cancer cell line (SUIT-2). Gastroenterol Jpn 1987; 22: 640-646.
[30] Tomlinson IP, Whyman A, Barrett JA and Kremer JK. Tumour marker CA15-3: possible uses in the routine management of breast cancer. Eur J Cancer 1995; 31A: 899-902.
[31] Yin BW and Lloyd KO. Molecular cloning of the CA125 ovarian cancer antigen: identification as a new mucin, MUC16. J Biol Chem 2001; 276: 27371-27375.
[32] Zhang L, Lv B, Shi X and Gao G. High expression of N-acetylgalactosaminyl-transferase 1 (GALNT1) associated with invasion, metastasis, and proliferation in osteosarcoma. Med Sci Monit 2020; 26: e927837.
[33] Hu Q, Tian T, Leng Y, Tang Y, Chen S, Lv Y, Liang J, Liu Y, Liu T, Shen L and Dong X. The O-glycosylating enzyme GALNT2 acts as an oncogenic driver in non-small cell lung cancer. Cell Mol Biol Lett 2022; 27: 71.
[34] Barkeer S, Chugh S, Karmakar S, Kaushik G, Rauth S, Rachagani S, Batra SK and Ponnusamy MP. Novel role of O-glycosyltransferases GALNT3 and B3GNT3 in the self-renewal of pancreatic cancer stem cells. BMC Cancer 2018; 18: 1157.
[35] Zhang Y, Du X, He Z, Gao S, Ye L, Ji J, Yang X and Zhai G. A Vanadium-based nanoplatform synergizing ferroptotic-like therapy with glucose metabolism intervention for enhanced cancer cell death and antitumor immunity. ACS Nano 2023; 17: 11537-11556.
[36] Wang YM, Gong FC, Qi X, Zheng YJ, Zheng XT, Chen Y, Yang ZT, Qing-Ye, Mao EQ and Chen EZ. Mucin 1 inhibits ferroptosis and sensitizes vitamin E to alleviate sepsis-induced acute lung injury through GSK3beta/Keap1-Nrf2-GPX4 pathway. Oxid Med Cell Longev 2022; 2022: 2405943.
[37] Zhao M, Li M, Zheng Y, Hu Z, Liang J, Bi G, Bian Y, Sui Q, Zhan C, Lin M and Wang Q. Identification and analysis of a prognostic ferroptosis and iron-metabolism signature for esophageal squamous cell carcinoma. J Cancer 2022; 13: 1611-1622.

[38] Tian Y, Liu H, Zhang C, Liu W, Wu T, Yang X, Zhao J and Sun Y. Comprehensive analyses of ferroptosis-related alterations and their prognostic significance in glioblastoma. Front Mol Biosci 2022; 9: 904098.
[39] Li HW, Liu MB, Jiang X, Song T, Feng SX, Wu JY, Deng PF and Wang XY. GALNT14 regulates ferroptosis and apoptosis of ovarian cancer through the EGFR/mTOR pathway. Future Oncol 2022; 18: 149-161.
[40] Stiegelbauer V, Vychytilova-Faltejskova P, Karbiener M, Pehserl AM, Reicher A, Resel M, Heitzer E, Ivan C, Bullock M, Ling H, Deutsch A, Wulf-Goldenberg A, Adiprasito JB, Stoeger H, Haybaeck J, Svoboda M, Stotz M, Hoefler G, Slaby O, Calin GA, Gerger A and Pichler M. miR-196b-5p regulates colorectal cancer cell migration and metastases through interaction with HOXB7 and GALNT5. Clin Cancer Res 2017; 23: 5255-5266.
[41] Rodrigues TC, Fidalgo F, da Costa CM, Ferreira EN, da Cunha IW, Carraro DM, Krepischi AC and Rosenberg C. Upregulated genes at 2q24 gains as candidate oncogenes in hepatoblastomas. Future Oncol 2014; 10: 2449-2457.
[42] Li Y, Zhu YY, Dai GP, Wu DJ, Gao ZZ, Zhang L and Fan YH. Screening and validating the core biomarkers in patients with pancreatic ductal adenocarcinoma. Math Biosci Eng 2019; 17: 910-927.
[43] Caffrey T, Sagar S, Thomas D, Lewallen ME, Hollingsworth MA and Radhakrishnan P. The glycoprotein mucin-1 negatively regulates GalNAc transferase 5 expression in pancreatic cancer. FEBS Lett 2019; 593: 2751-2761.
[44] Morad G, Helmink BA, Sharma P and Wargo JA. Hallmarks of response, resistance, and toxicity to immune checkpoint blockade. Cell 2022; 185: 576.
[45] Yuen VW, Chiu DK, Law CT, Cheu JW, Chan CY, Wong BP, Goh CC, Zhang MS, Xue HD, Tse AP, Zhang Y, Lau HY, Lee D, Au-Yeung RKH, Wong CM and Wong CC. Using mouse liver cancer models based on somatic genome editing to predict immune checkpoint inhibitor responses. J Hepatol 2023; 78: 376-389.
[46] Efimova I, Catanzaro E, Van der Meeren L, Turubanova VD, Hammad H, Mishchenko TA, Vedunova MV, Fimognari C, Bachert C, Coppieters F, Lefever S, Skirtach AG, Krysko O and Krysko DV. Vaccination with early ferroptotic cancer cells induces efficient antitumor immunity. J Immunother Cancer 2020; 8: e001369.
[47] Tang D, Chen X, Kang R and Kroemer G. Ferroptosis: molecular mechanisms and health implications. Cell Res 2021; 31: 107-125.
[48] Wang W, Green M, Choi JE, Gijon M, Kennedy PD, Johnson JK, Liao P, Lang X, Kryczek I, Sell A, Xia H, Zhou J, Li G, Li J, Li W, Wei S, Vatan L, Zhang H, Szeliga W, Gu W, Liu R, Lawrence TS, Lamb C, Tanno Y, Cieslik M, Stone E, Georgiou G, Chan TA, Chinnaiyan A and Zou W. CD8(+) T cells regulate tumour ferroptosis during cancer immunotherapy. Nature 2019; 569: 270-274.
[49] Liu B, Ji Q, Cheng Y, Liu M, Zhang B, Mei Q, Liu D and Zhou S. Biomimetic GBM-targeted drug delivery system boosting ferroptosis for immunotherapy of orthotopic drug-resistant GBM. J Nanobiotechnology 2022; 20: 161.
[50] Conche C, Finkelmeier F, Pesic M, Nicolas AM, Bottger TW, Kennel KB, Denk D, Ceteci F, Mohs K, Engel E, Canli O, Dabiri Y, Peiffer KH, Zeuzem S, Salinas G, Longerich T, Yang H and Greten FR. Combining ferroptosis induction with MDSC blockade renders primary tumours and metastases in liver sensitive to immune checkpoint blockade. Gut 2023; 72: 1774-1782.
[51] Song R, Li T, Ye J, Sun F, Hou B, Saeed M, Gao J, Wang Y, Zhu Q, Xu Z and Yu H. Acidity-activatable dynamic nanoparticles boosting ferroptotic cell death for immunotherapy of cancer. Adv Mater 2021; 33: e2101155.
[52] Hollingsworth MA and Swanson BJ. Mucins in cancer: protection and control of the cell surface. Nat Rev Cancer 2004; 4: 45-60.
[53] Fu J, Chen F, Lin Y, Gao J, Chen A and Yang J. Discovery and characterization of tumor antigens in hepatocellular carcinoma for mRNA vaccine development. J Cancer Res Clin Oncol 2023; 149: 4047-4061.
[54] Qiu P, Chen X, Xiao C, Zhang M, Wang H, Wang C, Li D, Liu J, Chen Y, Liu L and Zhao Q. Emerging glyco-risk prediction model to forecast response to immune checkpoint inhibitors in colorectal cancer. J Cancer Res Clin Oncol 2023; 149: 6411-6434.
[55] Vedunova M, Turubanova V, Vershinina O, Savyuk M, Efimova I, Mishchenko T, Raedt R, Vral A, Vanhove C, Korsakova D, Bachert C, Coppieters F, Agostinis P, Garg AD, Ivanchenko M, Krysko O and Krysko DV. DC vaccines loaded with glioma cells killed by photodynamic therapy induce Th17 anti-tumor immunity and provide a four-gene signature for glioma prognosis. Cell Death Dis 2022; 13: 1062.
[56] Liu Z, Liu B, Feng C, Li C, Wang H, Zhang H, Liu P, Li Z, He S and Tu C. Molecular characterization of immunogenic cell death indicates prognosis and tumor microenvironment infiltration in osteosarcoma. Front Immunol 2022; 13: 1071636.
[57] Chen AY, Wolchok JD and Bass AR. TNF in the era of immune checkpoint inhibitors: friend or foe? Nat Rev Rheumatol 2021; 17: 213-223.
[58] Dostert C, Grusdat M, Letellier E and Brenner D. The TNF family of ligands and receptors: communication modules in the immune sys-

tem and beyond. Physiol Rev 2019; 99: 115-160.
[59] Cao Y, Luo F, Peng J, Fang Z, Liu Q and Zhou S. KMT2B-dependent RFK transcription activates the TNF-alpha/NOX2 pathway and enhances ferroptosis caused by myocardial ischemia-reperfusion. J Mol Cell Cardiol 2022; 173: 75-91.
[60] Guo X, Hao Y, Ma H, Li H, Li L, Yan F, Huang J and Li L. The mechanism of monobutyl phthalate-induced ferroptosis via TNF/IL6/STAT3 signal pathway in TM-3 cells. J Toxicol Sci 2023; 48: 299-310.

Supplementary Table 1. The sequences of si-GALNT5

name	siRNA site	sense (5'-3')	antisense (5'-3')
si-GALNT5-1 (mix)	GALNT5-homo-586	GCCUCUCAUUCAGUGAGAUTT	AUCUCACUGAAUGAGAGGCTT
	GALNT5-homo-1270	GCAAAGAAGUCAAUGCAAATT	UUUGCAUUGACUUCUUUGCTT
	GALNT5-homo-2205	GCAGGAGCACAGAAUGCAATT	UUGCAUUCUGUGCUCCUGCTT
si-GALNT5-2 (mix)	GALNT5-homo-121	UAAGUUCUGAUAAACACUGGC	CAGUGUUUAUCAGAACUUAGC
	GALNT5-homo-1036	UCUAUCAGUACUAAGACUGAU	CAGUCUUAGUACUGAUAGACC
	GALNT5-homo-1236	AUAGAUUGCUUCCUUAAGCGA	GCUUAAGGAAGCAAUCUAUUA

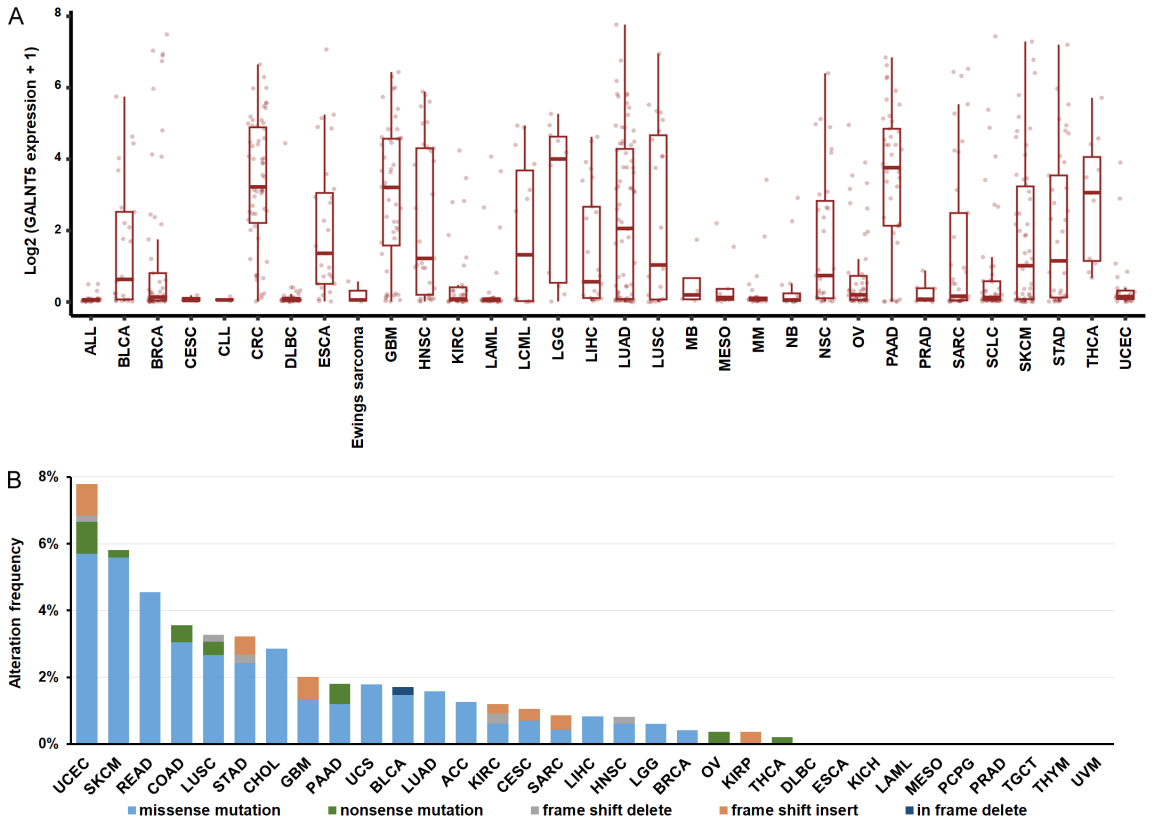

Supplementary Figure 1. Expression profile of GALNT5 in tumor cell lines and genomic alteration of GALNT5 in multiple tumors. A. Expression of GALNT5 across pan-cancer cell lines, according to the CCLE database. B. Types and frequency of genomic alterations in GALNT5 across multiple tumors, as per the TCGA database.

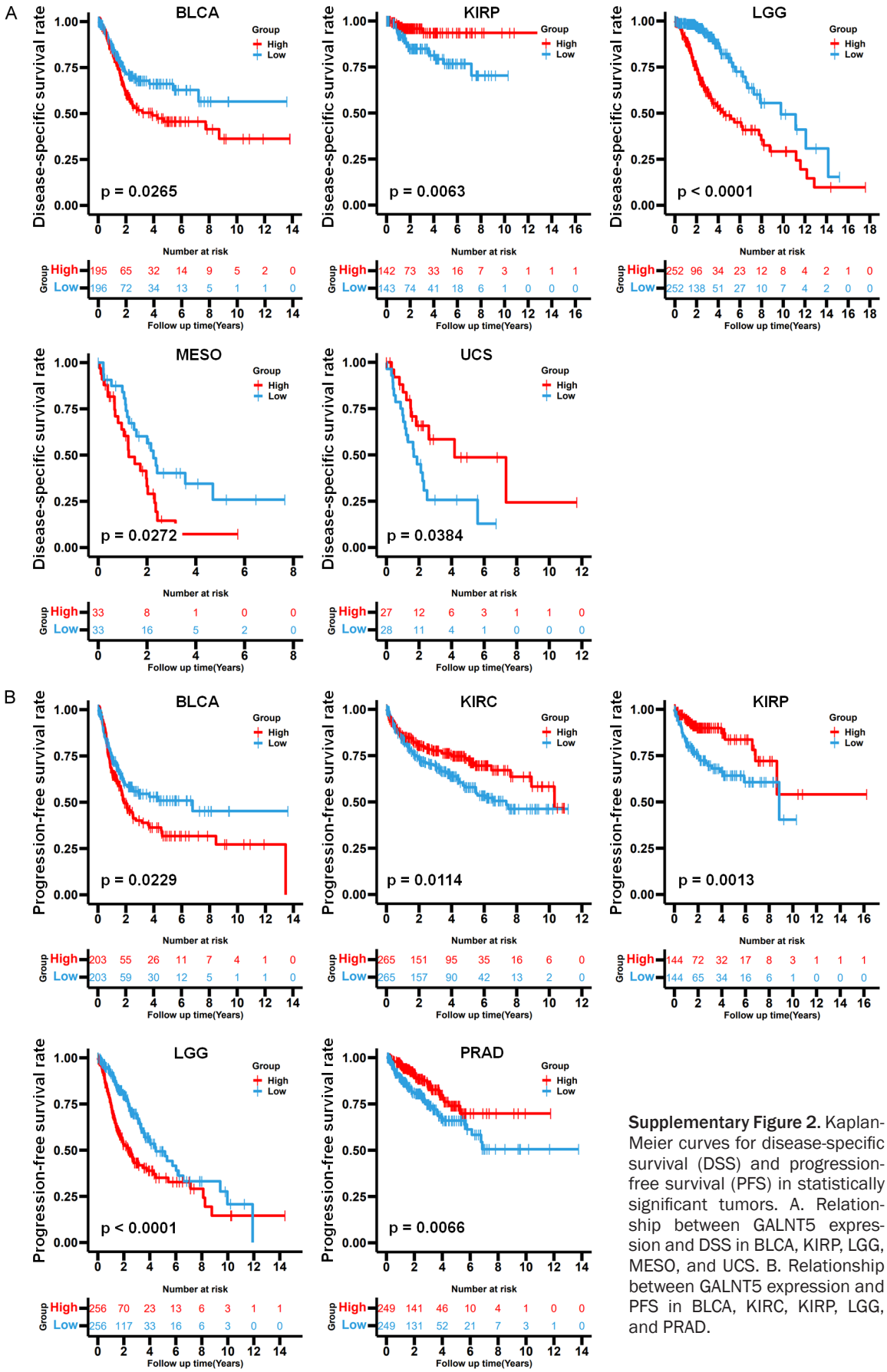

Supplementary Figure 2. Kaplan-Meier curves for disease-specific survival (DSS) and progression-free survival (PFS) in statistically significant tumors. A. Relationship between GALNT5 expression and DSS in BLCA, KIRP, LGG, MESO, and UCS. B. Relationship between GALNT5 expression and PFS in BLCA, KIRC, KIRP, LGG, and PRAD.

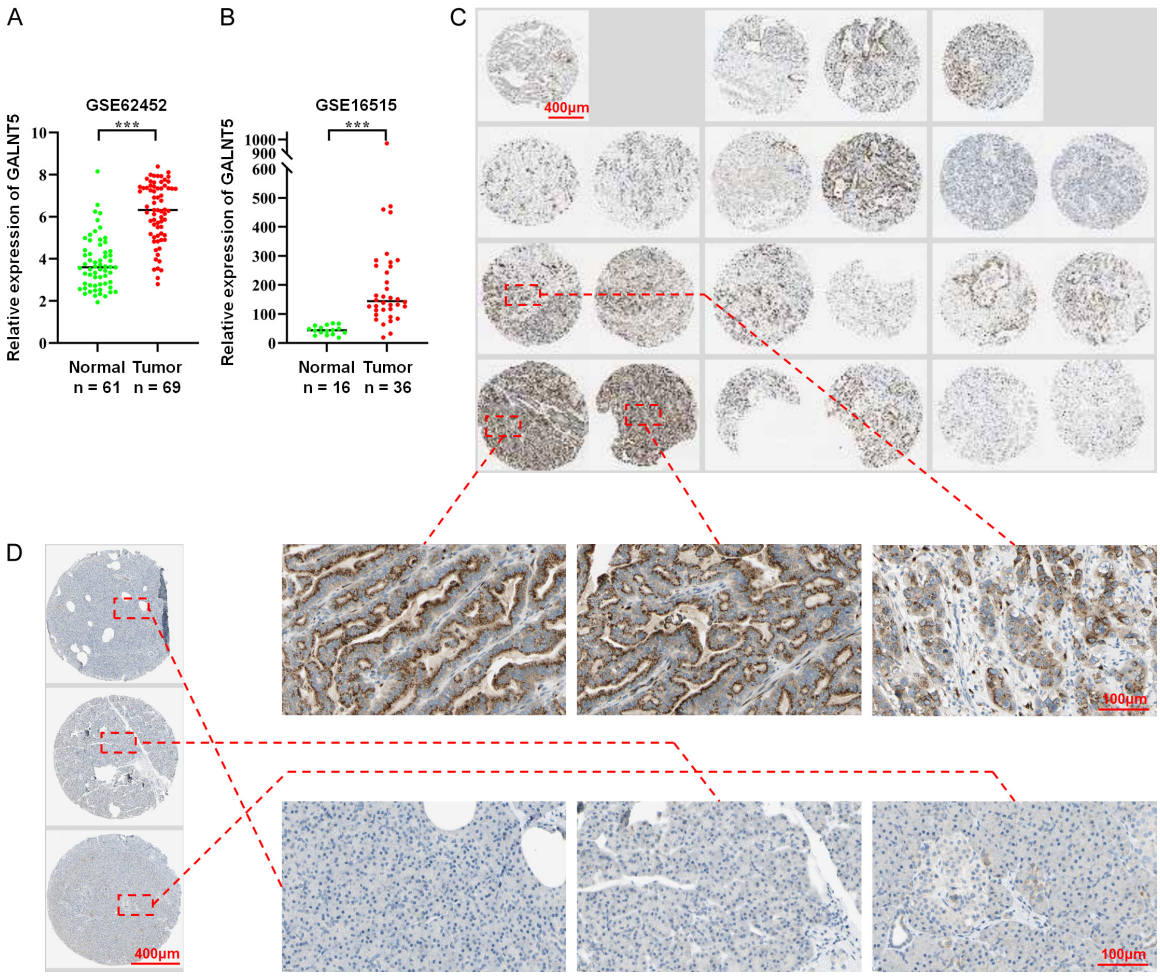

Supplementary Figure 3. Expression of GALNT5 in PAAD, based on GEO and HPA databases. A. Different expressions of GALNT5 between normal and PAAD tissues in GSE62452. B. Different expressions of GALNT5 between normal and PAAD tissues in GSE16515. C. The IHC staining of GALNT5 in PAAD tissues using the antibody HPA008693. D. The IHC staining of GALNT5 in normal pancreatic tissues using the same antibody. ***$P < 0.001$.

GALNT5 inhibits ferroptosis in PAAD

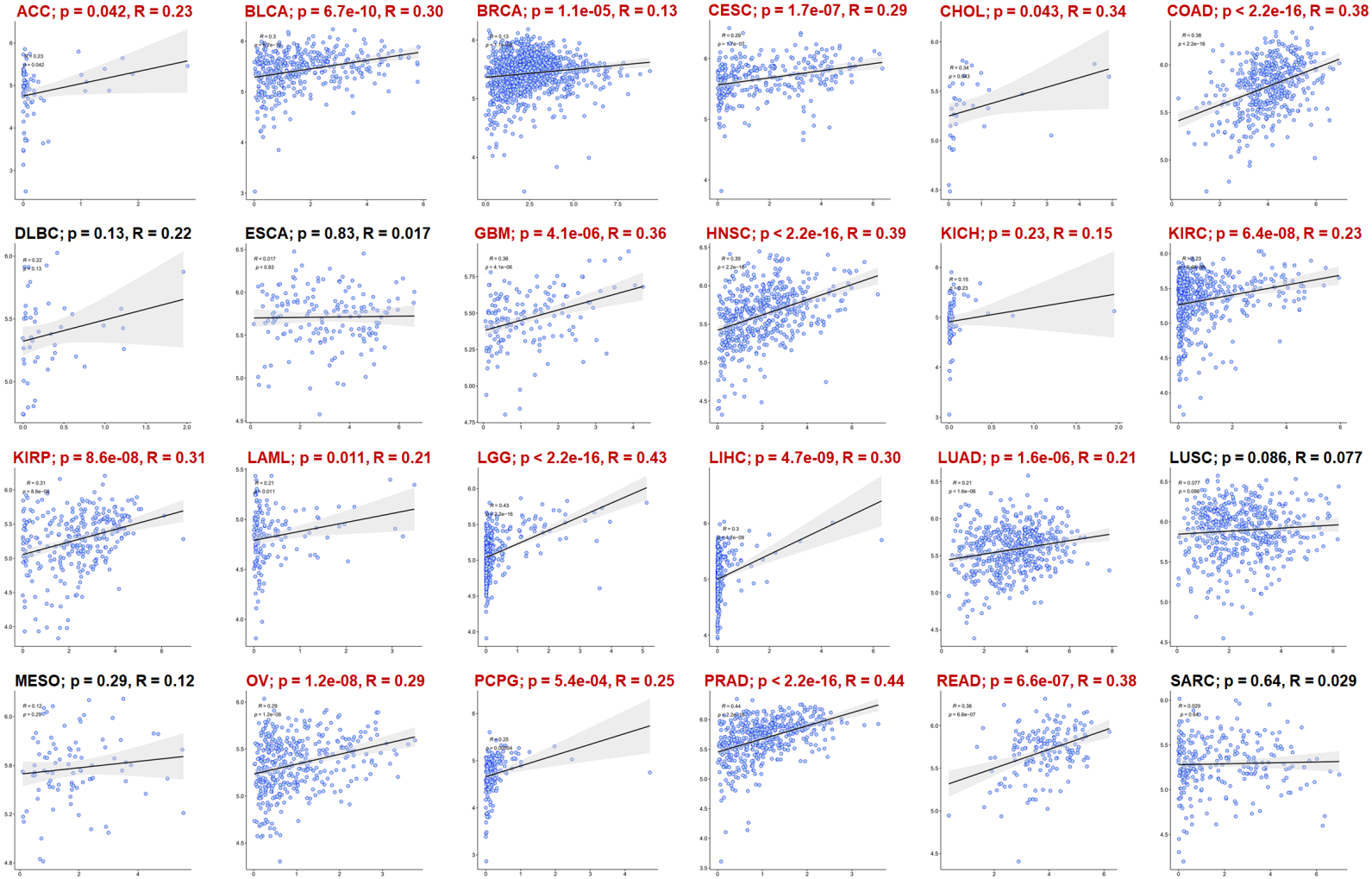

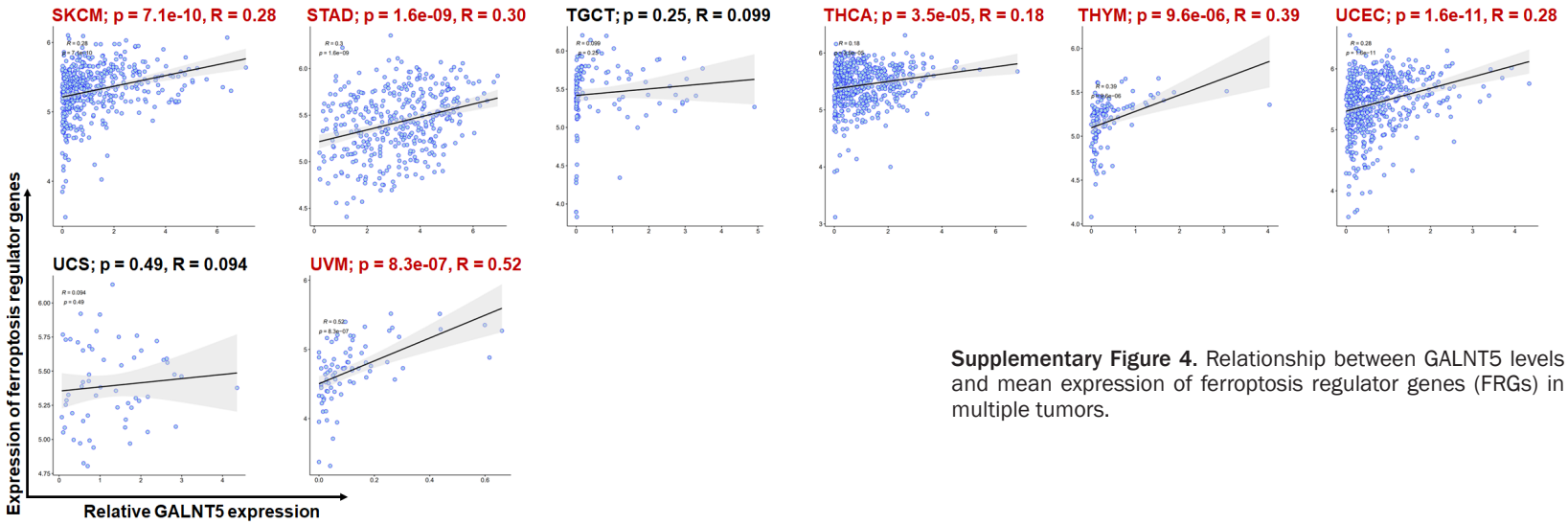

Supplementary Figure 4. Relationship between GALNT5 levels and mean expression of ferroptosis regulator genes (FRGs) in multiple tumors.

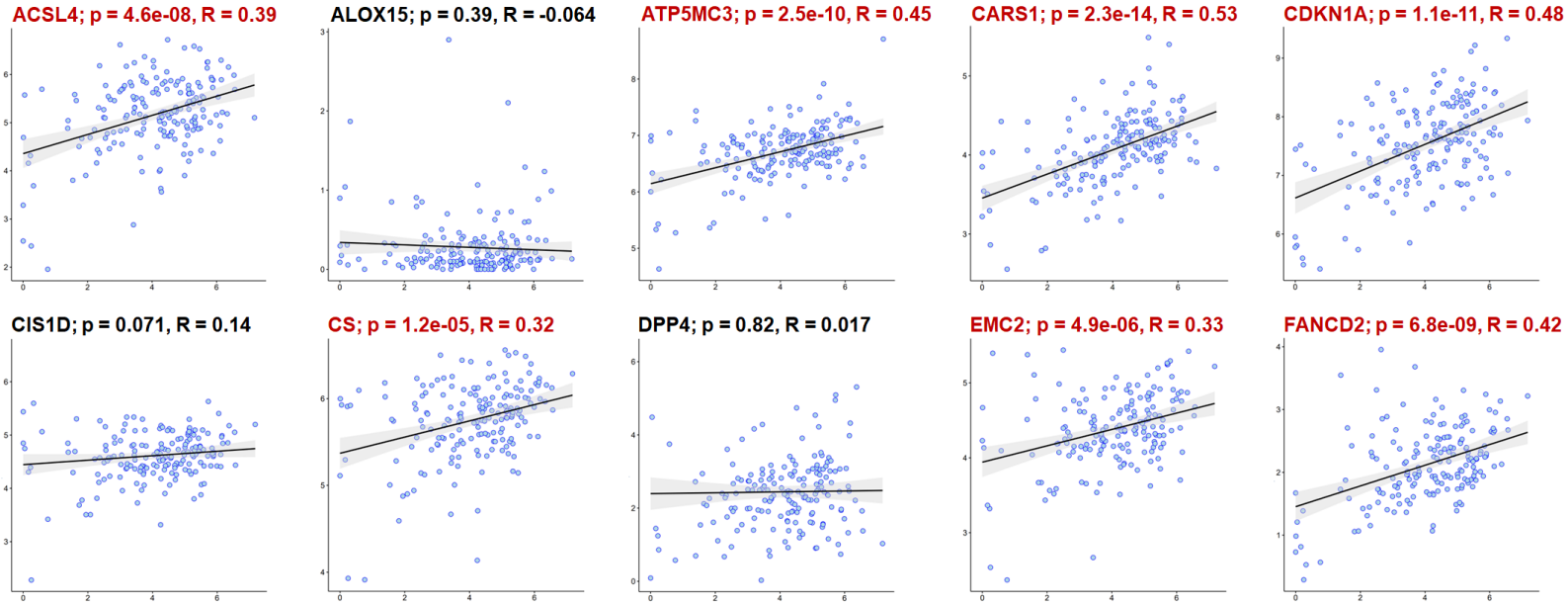

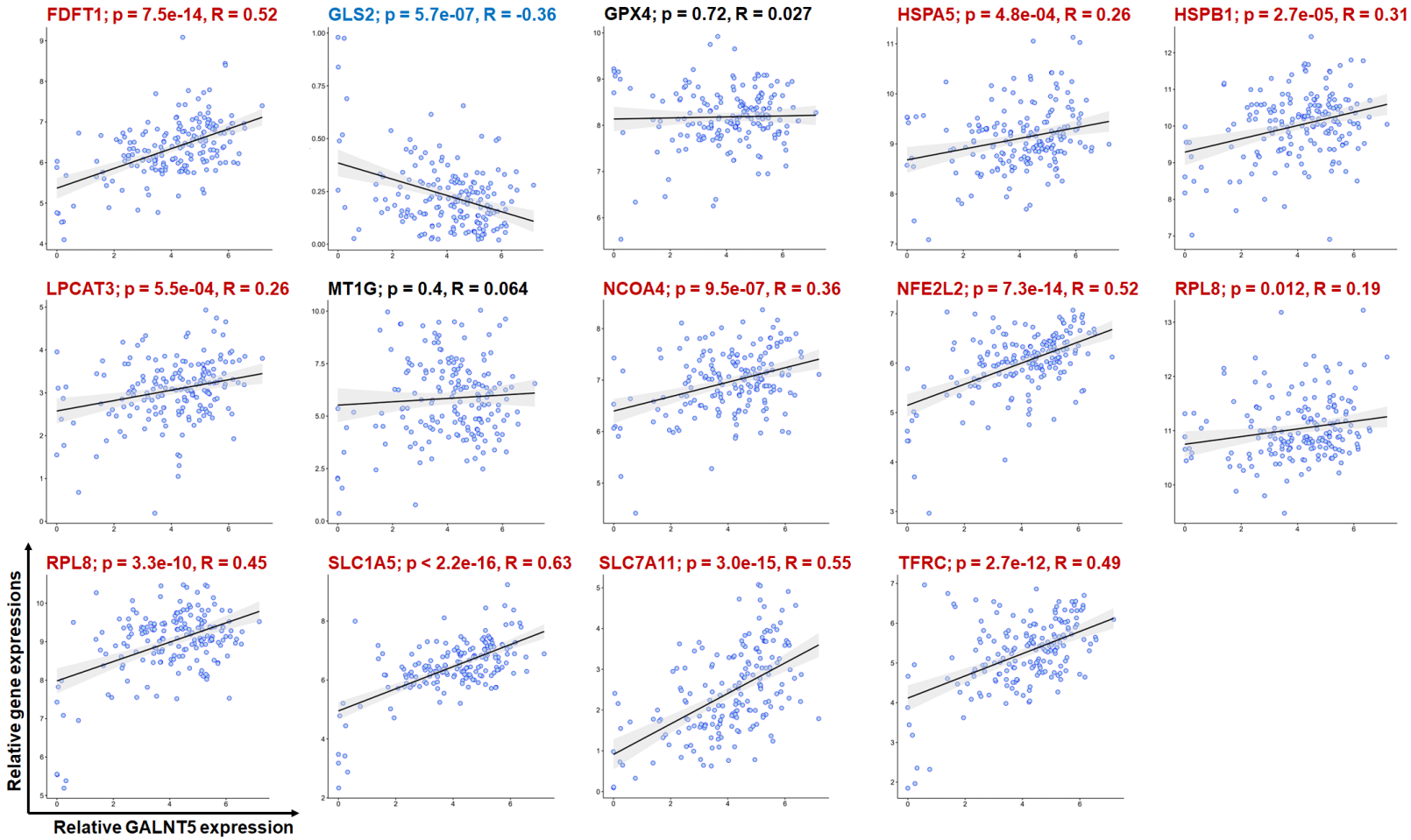

Supplementary Figure 5. Relationship between GALNT5 levels and each FRG expression in PAAD.

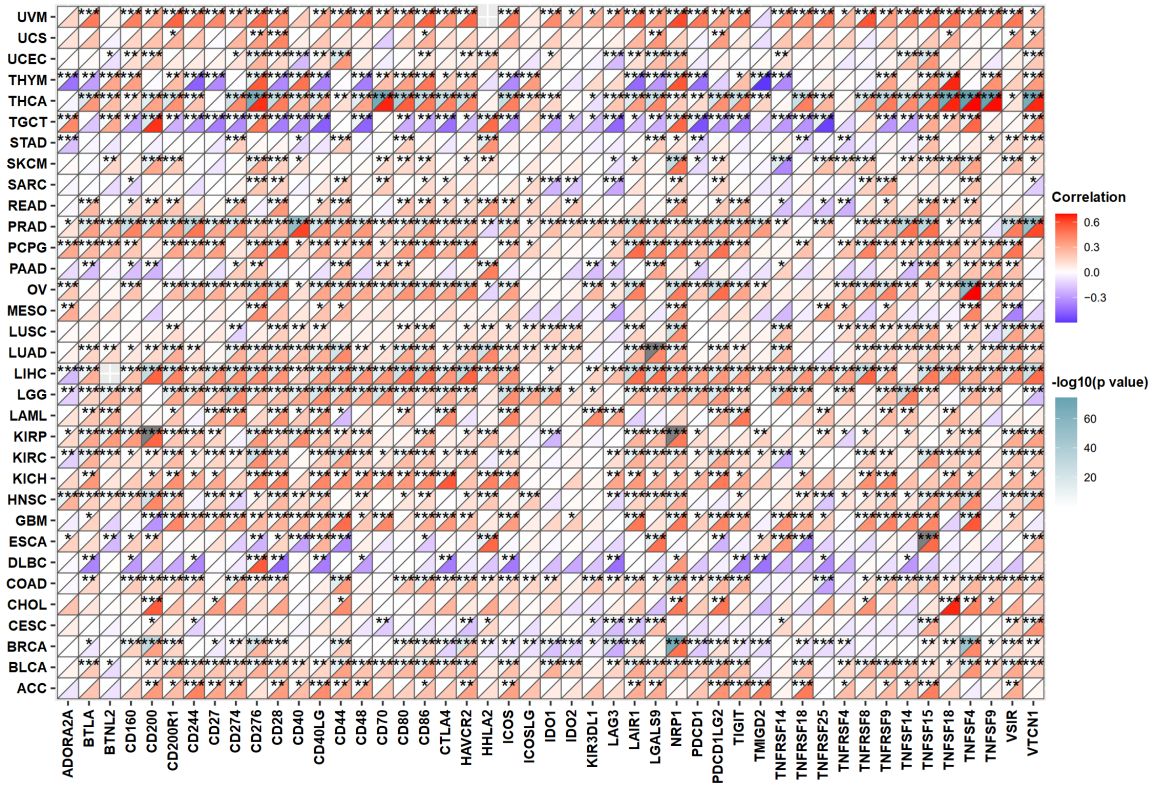

Supplementary Figure 6. Correlation of GALNT5 expression with immune checkpoint (ICP) genes in different tumors.

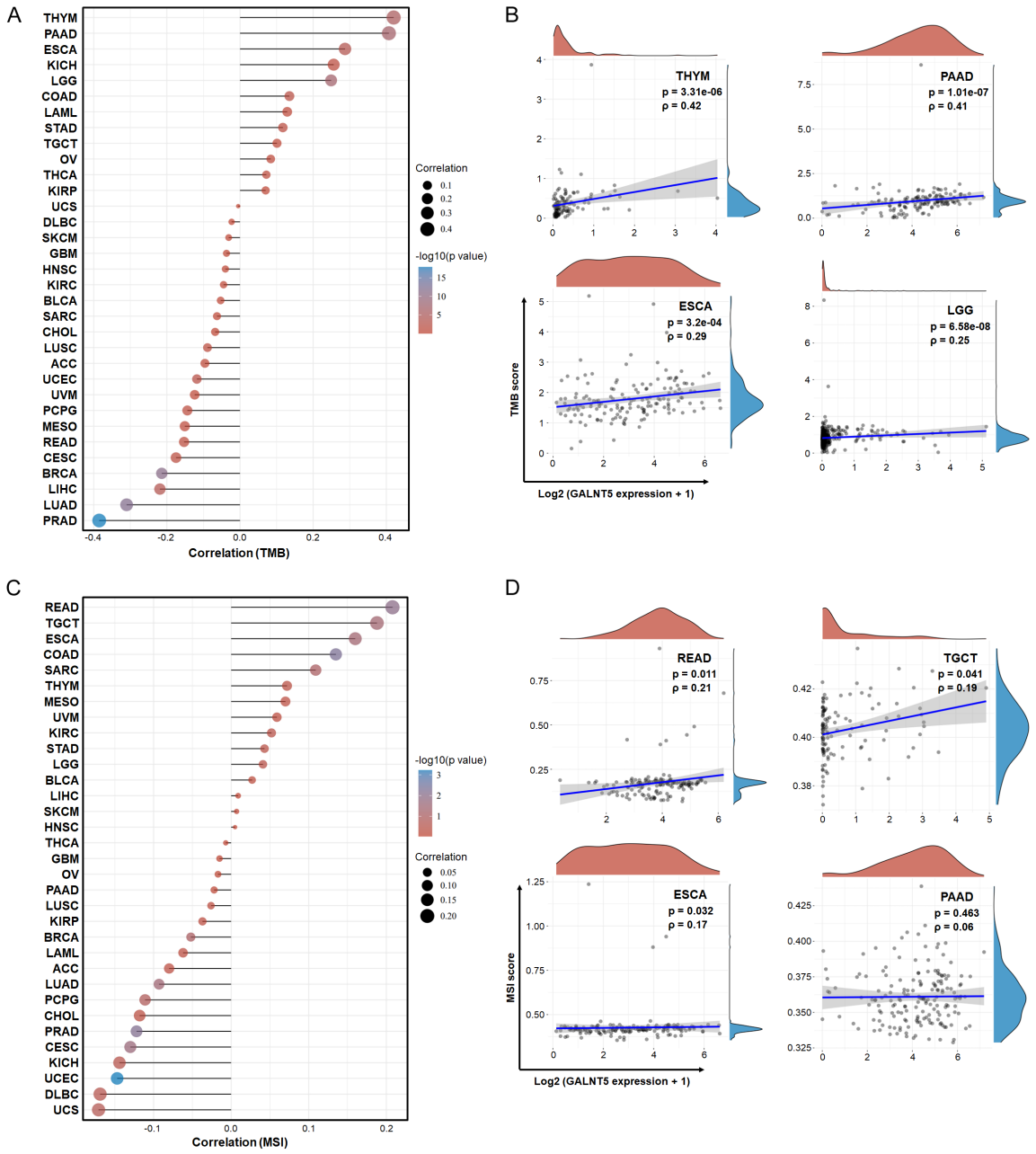

Supplementary Figure 7. Correlations of GALNT5 expression with tumor mutational burden (TMB) and microsatellite instability (MSI) across pan-cancers. A. Correlation between GALNT5 expression and TMB in various tumors. B. Association between GALNT5 level and TMB in THYM, PAAD, ESCA and LGG. C. Correlation between GALNT5 expression and MSI in various tumors. D. Association between GALNT5 level and MSI in READ, TGCT, ESCA and PAAD.

Supplementary Table 2. The correlations of GALNT5 expression with TMB and MSI in pan-cancers

Tumor types	TMB		MSI	
	Correlations	*p* value	Correlations	*p* value
ACC	-0.096	0.442	-0.08	0.522
BLCA	-0.053	0.289	0.027	0.591
BRCA	-0.214	8.44E-12	-0.052	0.090
CESC	-0.175	0.033	-0.13	0.024
CHOL	-0.068	0.699	-0.118	0.499
COAD	0.135	0.012	0.135	5.10E-03
DLBC	-0.023	0.896	-0.169	0.262
ESCA	0.287	3.37E-04	0.16	0.041
GBM	-0.037	0.656	-0.015	0.853
HNSC	-0.04	0.381	0.005	0.909
KICH	0.256	0.059	-0.144	0.290
KIRC	-0.045	0.402	0.052	0.345
KIRP	0.07	0.245	-0.037	0.531
LAML	0.129	0.195	-0.062	0.521
LGG	0.249	6.58E-08	0.041	0.377
LIHC	-0.219	4.21E-04	0.009	0.883
LUAD	-0.31	1.30E-12	-0.093	0.034
LUSC	-0.089	0.055	-0.026	0.565
MESO	-0.151	0.177	0.07	0.531
OV	0.084	0.183	-0.017	0.777
PAAD	0.407	1.32E-07	-0.022	0.774
PCPG	-0.144	0.061	-0.111	0.143
PRAD	-0.385	1.36E-18	-0.122	6.50E-03
READ	-0.153	0.094	0.208	0.011
SARC	-0.063	0.350	0.109	0.085
SKCM	-0.031	0.505	0.007	0.877
STAD	0.117	0.024	0.043	0.410
TGCT	0.101	0.287	0.188	0.041
THCA	0.072	0.115	-0.007	0.883
THYM	0.42	4.10E-06	0.072	0.439
UCEC	-0.118	7.86E-03	-0.147	6.15E-04
UCS	-0.005	0.971	-0.171	0.203
UVM	-0.124	0.289	0.059	0.616